BIOACTIVE POROUS PEG-PEPTIDE COMPOSITE HYDROGELS WITH TUNABLE MECHANICAL PROPERTIES

A THESIS

SUBMITTED TO THE MATERIALS SCIENCE AND NANOTECHNOLOGY PROGRAM OF GRADUATE SCHOOL OF ENGINEERING AND SCIENCE OF BILKENT UNIVERSITY

IN PARTIAL FULFILLMENT OF THE REQUIREMENTS

FOR THE DEGREE OF

MASTER OF SCIENCE

By

Melis Göktaş

August, 2014

I certify that I have read this thesis and that in my opinion it is fully adequate, in scope and in quality, as a thesis of the degree of Master of Science.

…….

Assoc. Prof. Dr. Mustafa Özgür Güler (Advisor)

I certify that I have read this thesis and that in my opinion it is fully adequate, in scope and in quality, as a thesis of the degree of Master of Science.

…….

Assist. Prof. Dr. Ayşe Begüm Tekinay

I certify that I have read this thesis and that in my opinion it is fully adequate, in scope and in quality, as a thesis of the degree of Master of Science.

…….

Assoc. Prof. Dr. Çağdaş Devrim Son

Approved for the Graduate School of Engineering and Science:

…….

Prof. Dr. Levent Onural

Director of the Graduate School

ABSTRACT

BIOACTIVE POROUS PEG-PEPTIDE COMPOSITE HYDROGELS WITH TUNABLE MECHANICAL PROPERTIES

Melis Göktaş

M.S. in Materials Science and Nanotechnology

Supervisor: Assoc. Prof. Mustafa Özgür Güler

August, 2014

Mimicking the instructive cues of native extracellular matrix (ECM) is fundamental to understand and control the processes regulating cell function and cell fate. Extensive research on the structure and biological complexity of ECM has shown that three types of critical information from the ECM have influence on cellular behaviour: (1) biophysical properties (elasticity, stiffness), (2) biochemical properties (bioactive peptide epitopes of ECM molecules), and (3) nanoarchitecture (nanofibrillar structure, porosity) of ECM. Recent efforts have therefore focused on the construction of ECM mimetic materials to modulate tissue specific cell functions. Advances in biomaterial platforms include artificial ECM mimics of peptide conjugated synthetic polymer hydrogels presenting bioactive ligands produced with covalent chemistry. These materials have already found application in tissue engineering, however, these biomaterial platforms represent oversimplified mimics of cellular microenvironment and lack the complexity and multifunctional aspects of native ECM.

In this work, we developed a novel polyethylene glycol (PEG)-peptide nanofiber composite hydrogel system with independently tunable biochemical, mechanical and physical cues that does not require any chemical modification of polymer backbone to create synthetic ECM analogues. This approach allows non-interacting modification of multifactorial niche properties (i.e. bioactive ligands, stiffness, porosity), since no covalent conjugation method was used to modify PEG monomers for the incorporation of bioactivity and porosity. Combining the self-assembled peptide nanofibers with crosslinked polymer network simply by facile mixing followed by photo-polymerization resulted in the formation of porous hydrogel systems. Resulting porous network can be functionalized with desired bioactive signalling epitopes by simply altering the amino acid sequence of peptide amphiphile molecules. In addition, the mechanical properties of the composite system can be precisely controlled by changing the PEG concentration. Ultimately, multifunctional PEG-peptide composite scaffolds reported in this work, can fill a critical gap in the available biomaterials as versatile synthetic mimics of ECM with independently tunable properties. Such a system could provide a useful tool allowing the investigation of how complex niche cues interplay to influence cellular behaviour and tissue formation both in 2D and 3D platforms.

Keywords: Extracellular Matrix (ECM), Peptide Nanofibers, Self Assembly, Polyethylene Glycol (PEG), Hydrogel

ÖZET

MEKANİK ÖZELLİKLERİ AYARLANABİLİR BİYOAKTİF POROZ PEG-PEPTİT KOMPOZİT HİDROJELLERİN ÜRETİMİ

Melis Göktaş

Malzeme Bilimi ve Nanoteknoloji Programı, Yüksek Lisans

Tez danışmanı: Doç. Dr. Mustafa Özgür Güler

Ağustos, 2014

Hücre davranışını ve hücre fonksiyonlarını düzenleyen mekanizmaların anlaşılması ve kontrol edilmesi amacıyla, doğal hücrelerarası matris ortamının yönlendirici özelliklerinin taklit edilmesi önem taşımaktadır. Doğal hücrelerarası matrisin yapısı ve biyolojik kompleksitesi üzerine yapılan çalışmalar hücrelerarası matrise ait üç tip kritik bilginin hücre davranışı üzerinde etkili olduğunu göstermiştir: (1) biyofiziksel özellikler (elastisite, sertlik), (2) biyokimyasal özellikler (biyoaktif peptit sinyalleri), ve (3) nanoyapı (nanofibriler yapı, porozite). Bu sebeple, günümüzde doku spesifik hücre davranışlarının yönlendirilmesi amacıyla gerçekleştirilen çalışmalar hücrelerarası matris ortamını taklit eden biyomalzemelerin geliştirilmesi üzerine odaklanmıştır. Biyomalzeme alanında en önemli yeniliklerden biri, kovalent kimya metotları kullanılarak biyoaktif peptit epitopları ile modifiye edilmiş sentetik polimer hidrojellerin geliştirilmesidir. Sentetik polimerler günümüzde doku mühendisliği alanında uygulama bulmalarına rağmen, bu malzemeler hücre mikro-ortamının oldukça basitleştirilmiş modelleri olarak kalmakta ve çok fonksiyonlu doğal hücrelerarası matrisin kompleks yapısını taklit edememektedirler.

Bu çalışmada, bağımsız olarak ayarlanabilir biyokimyasal, mekanik ve fiziksel özelliklere sahip özgün bir polietilen glikol (PEG)-peptit nanofiber kompozit hidrojel sistemi geliştirilmiştir. Geliştirilen kompozit hidrojel sistemi polimer yapısında herhangi bir kimyasal modifikasyona gerek duyulmaksızın sentetik ESM analoglarının üretimine olanak sağlamaktadır. Biyoaktivite ve porozitenin sağlanması için herhangi bir kovalent konjugasyon metodu kullanılmaması sayesinde üretilen hidrojellerin özellikleri birbirinden etkilenmeksizin çok yönlü olarak modifiye edilebilmektedir. Kendiliğinden biraraya gelen peptit nanofiberlerin, foto-polimerizasyon yöntemi ile çapraz bağlanan polimer ağı ile karıştırılması, porlu hidrojel sistemlerinin oluşturulmasını sağlamıştır. Elde edilen porlu yapılar basit bir şekilde peptit amfifil moleküllerinin amino asit dizilimleri değiştirilerek biyoaktif sinyallerle fonksiyonalize edilebilmektedir. Ayrıca oluşan kompozit sistemin mekanik özellikleri polimer konsantrasyonu değiştirilerek kolayca ayarlanabilmektedir. Sonuç olarak, üretilen çok fonksiyonlu PEG-peptit kompozit iskeleler doğal hücrelerarası matrisi taklit eden, özellikleri ayarlanabilir biyomalzeme platformları alanında önemli bir eksikliği giderebilecektir. Elde edilen bu sistem, iki boyutlu (2D) ve üç boyutlu (3D) ortamlarda hücrelerarası matris benzeri kompleks faktörlerin hücre davranışını ve doku oluşumunu nasıl etkilediğinin araştırılması için kullanışlı bir araç olarak işlev görebilir.

Anahtar kelimeler: Hücrelerarası Matris, Peptit Nanofiberler, Kendiliğinden Biraraya Gelme, Polietilen Glikol (PEG), Hidrojel.

ACKNOWLEDGEMENTS

I have spent two years in a great research environment with many valuable people. First of all, I would like to thank my supervisor Prof. Mustafa Özgür Güler for his support and guidance. He improved my scientific perspective and taught me to ask the right questions during my research. I also would like to thank Prof. Ayşe Begüm Tekinay for her guidance and support throughout my research. This work could not be accomplished without her precious contribution.

I would like to thank Hakan Ceylan, whose support and motivation contributed a lot to this work. I also want to thank Göksu Çınar for her companionship during two years.

I would like to thank Gülcihan Gülseren and Gülistan Tansık for always cheering me up and for their support. It was great to know you and work with you all: Melis Şardan, Reşad Mammadov, Aref Khalily, Ceren Garip, Elif Arslan, Didem Mumcuoğlu, Yasin Tümtaş, Öncay Yaşa, Gözde Uzunallı, Berna Şentürk.

I would like to thank UNAM (National Nanotechnology Research Center) for giving me this opportunity and TUBITAK (The Scientific and Technological Research Council of Turkey) for financial support, BIDEB 2228-A MSc fellowship, and grant 213M406.

Special thanks to my beloved family for their endless support and love…

TABLE OF CONTENTS

LIST OF ABBREVIATIONS

1D:	One-Dimensional
2D:	Two-Dimensional
3D:	Three-Dimensional
BET:	Brunauer-Emmett-Teller
BIS:	*N*,*N*′-methylenebis(acrylamide)
COL1:	Collagen-1
DDR:	Discoidin Domain Tyrosine Kinase Receptor
DIEA:	Diisopropylethylamine
ECM:	Extracellular Matrix
ESI:	Electrospray Ionization
FACIT:	Fibril Associated Collagens with Interrupted Triple Helices
FAK:	Focal Adhesion Kinase
FBS:	Fetal Bovine Serum
GAG:	Glycosaminoglycan
GAPDH:	Glyceraldehyde 3-Phosphate Dehydrogenase
HBTU:	*N*,*N*,*N*’,*N*’-Tetramethyl-O-(1*H*-benzotriazole-1-yl) Uranium Hexafluorophosphate
HPLC:	High Performance Liquid Chromatography
hMSCs:	Human Mesenchymal Stem Cells
ICC:	Immunocytochemistry
LC-MS:	Liquid Chromatography-Mass Spectrometry
LSA:	Limiting Strain Amplitude
LVR:	Linear Viscoelastic Range
MuSCs:	Skeletal Muscle Stem Cells

NSCs:	Neural Stem Cells
NHS:	*N*-Hydroxyl Succinimide
PA:	Peptide Amphiphile
PBS:	Phosphate Buffered Saline
PEG:	Polyethylene Glycol
PEGDA:	Polyethylene Glycol Diacrylate
PEGDMA:	Polyethylene Glycol Dimethacrylate
PNFs:	Peptide Nanofibers
PVA:	Polyvinyl Alcohol
qRT-PCR:	Quantitative Reverse Transcriptase Polymerase Chain Reaction
QSDFT:	Quenched Solid Density Functional Theory
Q-TOF:	Quadrupole Time of Flight
RUNX2:	Runt-Related Transcription Factor
SEM:	Scanning Electron Microscopy
SLPRS:	Short Leucine Rich Proteoglycans
TEM:	Tranmission Electron Microscopy
TFA :	Trifluoroacetic Acid
UV :	Ultraviolet
vmIPN :	Interpenetrating Networks with Variable Moduli

LIST OF FIGURES

LIST OF TABLES

CHAPTER 1

INTRODUCTION

CHAPTER 1

1.INTRODUCTION

1.1. MICROENVIRONMENT OF CELLS: EXTRACELLULAR MATRIX

Cellular reactions are guided by the highly complex microenvironment of cells and the fate of cells is determined by information received from soluble factors, other cells, and the physical network they are encapsulated in. This physical network that provides structure and support to cells is called extracellular matrix (ECM). Cells secrete ECM molecules and maintain the matrix through continuous remodeling of its structure. ECM in turn, provides support to cells to communicate with each other and with the external environment. [1-2]

For many years, ECM was known as an inert background which occupies the space between the cells to provide a physical network for structural support. However, recent investigations have clarified that ECM is much more complex than it was thought to be and acts as an active component for the control of cell behaviour.[3-5] It is now accepted that, beginning with embryogenesis and continuing through adulthood, cellular development is influenced by the interaction between cells and their ECM.[6] Along with its heterogeneous composition that consists of proteins, proteoglycans, and signalling molecules, ECM is a supply of complex information for cells. Information contained in the ECM provides cells temporal and positional clues such as where they are, where they should be going, how old they are (in terms of cellular differentiation), and

when it is time for to die (apoptosis).[7] Biochemical (cell adhesion, presentation of signalling molecules) and mechanical (stiffness, remodelling) properties of ECM provided by its macromolecular components and bioactive cues can directly influence cell survival, proliferation, migration and differentiation.[8-9] Thus, successful understanding of ECM structure and signals can provide us the ability to evaluate complex intracellular signalling pathways and control cellular functions.

1.2. ECM STRUCTURE AND FUNCTION

ECM consists of a great diversity of insoluble macromolecules including structural proteins such as collagens and elastin, glycoproteins including fibronectin, vitronectin and laminin, and glycosaminoglycans.[10] Fibrous ECM proteins form a network of fibers and fibrils. Composition and spatial arrangement of ECM can vary from one tissue type to another. For example, bone ECM is mostly composed of collagen type I, and non-collagenous proteins including osteocalcin, fibronectin and vitronectin while cartilage ECM mostly consists of collagen type II and aggrecans.[11-13] Since, different ECM macromolecules can selectively stimulate different signalling pathways through cell-ECM interactions, this tissue-specific composition of ECM might be instructive for materials science to regulate cell behaviour to obtain the desired output.

1.2.1. Macromolecular Components of ECM

1.2.1.1. Collagen

Collagen is the most abundant component of the ECM and it forms ~30% of the total proteins in the body.[14] Collagen provides tensile strength and elasticity to tissues and organs, and it forms the structural framework of connective tissues including bone, tendons and dermis.[15-16]

Collagens are characterized by a distinct triplet of amino acid repeat defined as Gly-X-Y that eventually forms a triple helix structure. Gly represents glycine amino acid, while X and Y residues can be any amino acid but are commonly proline and hydroxyproline.[17] Each single polypeptide chain forming the triple helical assembly is called α-chain and collagens are separated according to the composition of α-chains and their supramolecular assembly. According to the repeat length and integrity of the Gly-X-Y repeats, self-assembly of the α-chains may result in the formation of uninterrupted triple helix structure as in the case of fibrillar collagen or the presence of the non-collagenous domain can form helical interruptions. Therefore, different α-chain motifs give rise to a number of different supramolecular assemblies with various geometric networks.[18] For example, in skin, tendon, bone and cartilage, the collagenous backbone of the ECM consists of crossbanded fibril-forming collagens (Type I, II, III, V, XI, XXIV, and XXVII) and the structure is supported by fibril-associated collagens with interrupted triple helices (FACIT) (Type IX, XII, XIV, XVI, XX, andf XXI) as well as microfibrillar type VI collagen.[19-21] Some other collagen types like network forming collagens (Type IV, VII, and X) contain large collagenous

domains interrupted by short non-collagenous sequences (other than Gly-X-Y repeat). Type IV collagens which are found in the basement membrane of epithelial tissues assemble into chicken-wire-like collagenous networks, while the ones found in the Descemet's membrane of the eye (Type VIII) and hypertrophic cartilage (Type X) forms regular hexagonal networks.[22-24] This structural heterogeneity provides different organization of collagen types within the ECM of different tissues with functional diversity and contributes to a range of biological functions including cell adhesion, migration, tissue repair, molecular filtration and tumor suppression.[25]

1.2.1.2. Adhesive Glycoproteins

Cells adhere to ECM through interaction with adhesive glycoproteins including fibronectin, vitronectin, laminin, thrombospondins, tenascins, entactins, nephronectin, fibrinogen, and others. Adhesive glycoproteins bind to cells through cell surface integrin receptors and interact with other ECM proteins to form a complex matrix network. Interactions between the cells and ECM glycoproteins can alter many cellular responses such as survival, growth, migration and differentiation. In this section, major cell adhesion proteins namely fibronectin (which interacts with more than ten different integrin receptors), vitronectin, and laminin are discussed.

1.2.1.2.1. Fibronectin

Fibronectin is a high molecular weight dimeric glycoprotein (~450 kDa per dimer) which is expressed by a variety of cells.[26] Some forms of fibronectin such as the ones found in blood plasma can remain in soluble form, while the ones found in the ECM are associated into disulfide-bonded fibrillar form.[7] ECM fibronectin consists of two similar subunits with a molecular weight of ~220 to 250 kDa covalently linked through disulfide bonds near the C-terminus.[27] Each fibronectin subunit contains three types of repeating modules defined as FN1 (12 type I repeats), FN2 (2 type II repeats), and FN3 (15-17 type III repeats). These modules form 90% of the total sequence. The remaining part includes a connector between $_5$FN1 and $_6$FN1 modules, a connector between $_1$FN3 and $_2$FN3 modules, and a variable (V) sequence (Figure 1).[28] Each fibronectin molecule contains binding sites of a variety of molecules including cell surface integrins ($\alpha_5\beta_1$, $\alpha_V\beta_1$, $\alpha_V\beta_3$, $\alpha_V\beta_5$, $\alpha_V\beta_6$, $\alpha_3\beta_1$, $\alpha_4\beta_1$, $\alpha_4\beta_7$, $\alpha_8\beta_1$, $\alpha_{IIb}\beta_3$) collagens, proteoglycans and heparin sulfate. Therefore, fibronectins provide binding sites to cells, also serve to bind other components of the ECM together.

1.2.1.2.2. Vitronectin

Vitronectin (also known as serum spreading factor, S-protein, and epibolin) is a multifunctional glycoprotein found in blood plasma and ECM.[29] It is found in the fibrillar form in ECM of a variety of tissues and colocalizes with fibronectin and elastic fibers.[7] Vitronectin can also interact with a variety of ECM molecules including collagen and heparin as well as some cell surface integrins ($\alpha_{IIb}\beta_3$, $\alpha_v\beta_1$, $\alpha_v\beta_3$, $\alpha_v\beta_5$, $\alpha_v\beta_8$, $\alpha_8\beta_1$).[30-34] However, $\alpha_5\beta_1$, which is the major integrin receptor for

fibronectin, does not recognize vitronectin. Interactions between vitronectin and integrin receptors of cells activate intracellular signalling pathways to mediate cellular functions such as adhesion, spreading, migration, differentiation, growth and apoptosis.[35-38]

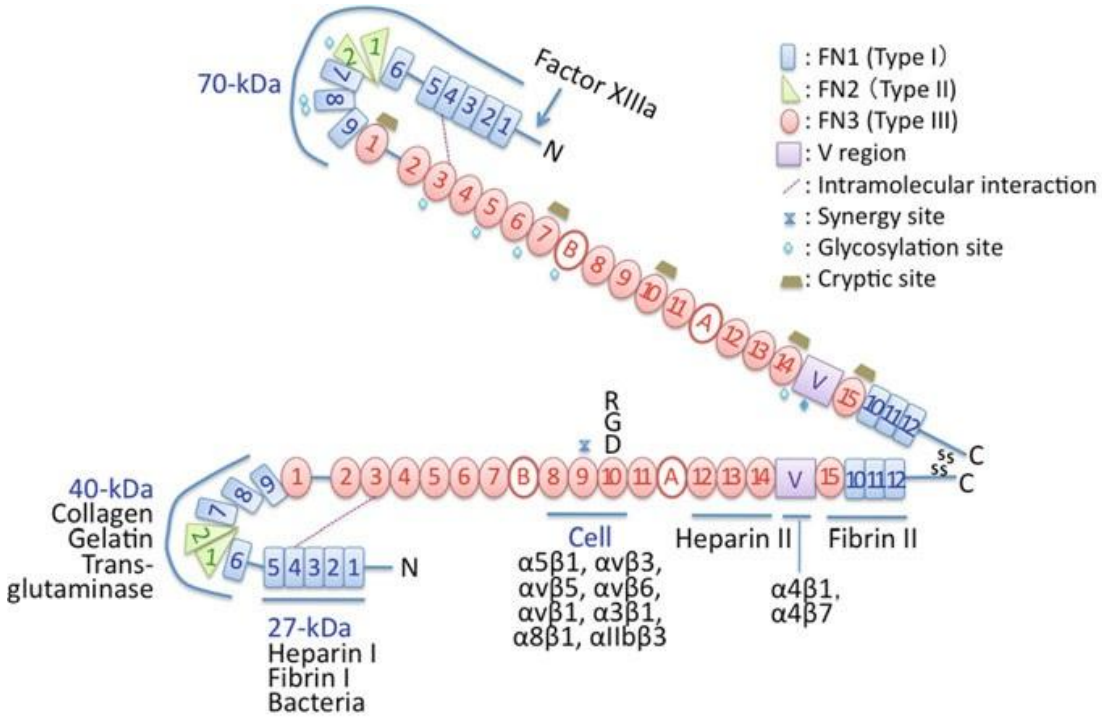

Figure 1.1. Diagram of fibronectin modular structure, structure of fibronectin modules and binding units (Reproduced with permission from ref. 28, copyright © Springer.).

1.2.1.2.3. Laminin

Laminins are large adhesive glycoproteins (400-900 kDa) that consist of three different polypeptide chains (α, β and γ) which form its heterotrimeric structure. Laminin binds to cell surface receptors such as integrins, heparins and α-

dystroglycan.[28] Majority of the binding sites for integrin receptors are found on the long α-chain of the laminin molecule. Most of the integrin receptors that have been reported to bind laminin are found in the integrin β_1 family including $\alpha_1\beta_1$, $\alpha_2\beta_1$, $\alpha_3\beta_1$, $\alpha_6\beta_1$, $\alpha_6\beta_4$, $\alpha_7\beta_1$, and $\alpha_9\beta_1$ integrins. Other integrins that bind to laminin include $\alpha_v\beta_3$ and $\alpha_6\beta_4$.[39-40] Interaction of the laminin with integrin receptors activates different intracellular signalling pathways involving focal adhesion kinases (FAK), mitogen-activated protein kinases (MAPK), phosphatases, and cytoskeletal components. Along with the signal transduction, cellular behaviours such as survival, adhesion, migration, proliferation and differentiation can be mediated by laminin-integrin interactions.[41-44]

1.2.1.3. Matricellular proteins and proteoglycans

Matricellular proteins function by binding to other matrix proteins and cell surface receptors, however they do not make any contribution to the structural integrity of the ECM.[45] Members of matricellular proteins include thrombospondins, tenascins, osteonectin and osteopontin.[7] Even though they are referred as "anti-adhesive proteins", since they induce rounding and detachment of some cells *in vitro*, they also act as regulators of cell adhesion, migration and differentiation in various tissues.[10]

Proteoglycans contain a number of families of multidomain proteins that are covalently attached to glycosaminoglycan (GAG) chains. Proteoglycans are named according to the type of attached GAG chains. Large proteoglycans such as aggrecan, versican, neurocan and brevican are able to form very-high-

molecular-weight aggregates by interacting with hyaluronate.[46] The interaction between hyaluronate and highly sulfated, negatively charged GAG side-chains of large proteoglycans provides the turgor and elasticity of many tissues.[47] For example, in cartilage, large hyaluronan-aggrecan complexes are entrapped within the fibrillar collagen network and the high-content of sulfated GAGs provide the high water uptake capacity of the tissue.[48] Therefore, cartilage tissue can generate enormous turgor and elasticity, and shows great mechanical resistance to pressure.[46]

Besides large pretoglycans, another protein family called short leucine rich proteoglycans (SLPRS), which includes decorin, biglycan, fibromodulin, chondroadherin, and aspirin, plays an important role in collagen fibril assembly as well as the storage and inhibition of transforming growth factor β and bone morphogenetic proteins.[49-50] Thus, even tough proteoglycans do not support cell adhesion and growth directly, they indirectly affect cell behavior as the regulators of extracellular matrix assembly, providers of tissue resilience and modulators of growth factors.[51]

1.3. CELL-ECM INTERACTIONS

Several types of receptor families including integrins, syndecans and discoidin-domain tyrosine kinase receptors DDR1 and DDR2, take roles in the recognition of signals coming from the ECM.[52] However, the transmission of chemical and mechanical signals from the ECM is primarily mediated by integrin receptors.[53]

Integrins are heterodimeric transmembrane receptors that provide the connection between ECM and cytoskeleton of cells. Each integrin receptor consists of α and β subunits. Up to date, 18 α and 8 β integrin subunits have been identified and various combination of these subunits were found lead to formation of 24 different heterodimers, which have unique binding characteristics determining the ligand specifity.[54]

Most of the integrins can bind to several types of ECM molecules, and one ECM molecule can bind to more than one integrin. Major ECM binding integrins include β_1 integrin that are able to bind to fibronectin ($\alpha_4\beta_1$, $\alpha_5\beta_1$, $\alpha_5\beta_3$, $\alpha_v\beta_3$), collagen ($\alpha_1\beta_1$, $\alpha_2\beta_1$, $\alpha_{10}\beta_1$, $\alpha_{11}\beta_1$) and laminins ($\alpha_3\beta_1$, $\alpha_6\beta_1$, $\alpha_7\beta_1$).[55]

Both α and β subunits, which pass through the cell membrane have large (700-1100 residues) extracellular domains and small (30-50 residues) cytoplasmic domains. The extracellular domains of integrins recognize their target ligand. Upon binding, conformational changes in the integrin molecules occur and their cytoplasmic domains associate with cytoskeleton and intracellular signal transduction molecules.[56-58] Binding of the intracellular integrin domains to focal complex proteins including focal adhesion kinase FAKp130, integrin-linked kinase, Fyn and c-src is followed by the incorporation of intracellular proteins such as paxillin, α-actinin, vinculin, talin, and zyxin into the focal complexes.[59-61] Association of the integrins with this complex signalling network activates downstream signalling cascades such as protein kinase C, Rac, Rho and MAPK pathways.[61-62] Along with the signalling, clustering of ECM ligands, integrins and

cytoskeletal components including actin fibers lead to formation of focal adhesions.[63] Depending on the regulated specific signalling pathway within the cells, integrin mediated cell-ECM interactions can alter cellular behaviours such as survival, proliferation and differentiation.[64-66] Therefore, elucidation of cell-ECM interactions and utilization of integrin binding epitopes can be a useful target for biomimetic tissue engineering strategies.

1.3.1. Adhesive properties of ECM: Integrin-binding epitopes

Although ECM macromolecules such as collagens, fibronectin, vitronectin and laminin have long protein backbones, integrin binding is very specific and integrins recognize only a few short peptide sequences within the molecules. One of the most studied integrin-binding epitopes is RGD-adhesive peptide sequence found in fibronectin, vitronectin, laminin and other adhesive glycoproteins.[67] Even tough it was first discovered in vitronectin, RGD sequence is well-known for its binding to $\alpha_v\beta_3$ integrins that recognize the sequence located in the 3rd repeat of FN3 domain in fibronectin.[68-69] RGD peptide motif is also found within the typical Gly-X-Y-Gly-X-Y order of collagen molecules, however most of these sequences lack of bioactivity. One of the active forms is found in type IV collagen and the three aminoacids forming the R-G-D sequence is located in the separate α chains of the collagen molecule, which is recognized by $\alpha_v\beta_3$ integrins.[70] Another well-known integrin-binding peptide sequence found in the collagens is GFOGER sequence, which has been located in type I collagen. [71] GFOGER sequence binds to β_1 family of integrins, including $\alpha_1\beta_1$, $\alpha_2\beta_1$, $\alpha_{10}\beta_1$, with a high affinity.

Also, RGD sequences located in the α1 and α2 chains of the laminin molecule have been found to be adhesive and they are recognized by $\alpha_6\beta_1$ and $\alpha_7\beta_1$ integrins.[72-73] Other studies have identified another short peptide sequence YIGSR located in the β1 chain of laminin responsible for integrin-mediated cell adhesion and differentiation.[74-75] α1 chain of the laminin contains another adhesive sequence IKVAV which promotes cell adhesion, migration, neurite outgrowth and tumor growth.[76]

Apart from these extensively studied adhesive sequences, some other integrin-binding epitopes were identified in fibronectin (REDV[77], LDV[78] and PHSRN[79]), collagen (DGEA[80]) and laminin (PDSGR[81]).

1.3.2. Mechanical properties of ECM

Collagen and elastin are the two major structural proteins of the native ECM. Mechanical properties of ECM are determined by a complex structure constructed by interwoven fibers of collagen and elastin proteins in a diameter from 10 to hundreds of nanometers.[82] Naturally, elastin is a highly elastic ECM protein that can stretch up to 2-3 times of its original length and turn back to its initial position with a minimum energy loss.[83] On the other hand, collagen is about 100 times stiffer than elastin and it is almost inextensible.[84] The amounts and organization of these two proteins within the ECM determine the mechanical stiffness of different native tissues which can vary significantly throughout the body (for example, brain: ~ 0.2-1 kPa, muscle: ~ 10 kPa, osteoid: ~ 30-45 kPa).[85-88] Other insoluble proteins including fibronectin and laminin are located on this

mechanical backbone to provide specific binding epitopes to integrin receptors of cells. These interactions make it possible for cells to sense the physical features of their microenvironment.[82] Therefore, cells are not only sensitive to adhesive properties of ECM but also to its mechanical properties. They can sense the mechanical stiffness of their environment, and as a response to perceived mechanical stimuli, they generate biochemical activity through the signal tranduction mechanism called mechanotransduction.[89-90] Associated with mechanical signal transduction, matrix stiffness can regulate cellular functions including adhesion[91], spreading[92], migration[93], proliferation[94] and differentiation[95-96].

1.3.2.1. Cell probing of ECM stiffness: Mechanotransduction

Many of the integrins are found in focal adhesion plaques, which are sites of high concentrations of various cytoskeletal proteins, and they are involved in various aspects of cell-cell and cell-ECM interactions, which are critical for cell behavior, specifically cell adhesion, migration, survival, and differentiation. Extracellular domains of integrins bind to specific peptide sequences in ECM, while intracellular domains connect to the cytoskeleton through focal adhesions that contain actin related proteins such as talin, vinculin, paxillin, and zyxin.[97] They regulate cytoskeletal organization and mediate transmembrane signal transduction. ECM-integrin interaction leads to the reorganization of the actin cytoskeleton, initiation of signal transduction cascades and coordination of responses to growth factors. The cytoplasmic domains of integrin subunits are required for these functions.[98] Indeed, the β1 integrin cytoplasmic domain has

been shown to contain all the information required for its localization to focal adhesion plaques, [99,100,101] and for the initiation of many of the integrin-mediated signalling events,[100,101] although the cytoplasmic domains of the α subunits can modify some of these parameters.[102]

When a mechanical stress is applied to a tissue, force is transferred over the ECM and channeled to microfilaments, microtubules and intermediate filaments of cytoskeleton through integrins.[103] Resulting rearrangement of cytoskeletal filaments comprise shape changes in the molecules associated to cytoskeleton. This shape change alter the biophysical properties (thermodynamics, kinetics) and biochemistry (chemical reaction rates) of the molecules.[104] Enzymes, substrates and many signal transduction molecules such as ion channels, protein kinases, G proteins, small GTPases and growth factors, oriented on the integrin binding sites of cytoskeletal backbone, regulate cellular metabolism according to these changes.[105] Force tranmission through integrins and cytoskeletal filaments concentrates stress not only on focal adhesions but also organelles at the distant sites of cytoplasm and nucleus.[106] Forces transferred to nucleus through the cytoskeleton may also effect gene regulation by activating stress-sensitive ion channels on nuclear membrane and altering nucleolar function, chromatin folding, and access to transcription factors. Thus, mechanotransduction at cellular level not only defines the cell morphology but also regulates gene transcription and differentiation.[107]

1.3.3. Nanostructure and porosity of ECM

In addition to its adhesive and mechanical properties, architectural cues of the native ECM are also important for the modulation of cellular behaviour. To maintain metabolic activity, cells need to receive nutrients and remove the metabolic waste. Therefore, cells require an permeable ECM environment that allows the diffusion of nutrients and waste products.[6] Thus, porosity of the ECM is crucial to provide diffusion and it affects the cellular processes. A compact ECM with high cell density and dense composition can reduce the nutrient diffusion into the interior layers of tissues and ejection of the waste compounds as in the case of solid tumors, which develop necrotic cores due to poor diffusion.[108]

Porosity is also important for the regulation of cell function. In each individual natural tissue, porosity and permeability of the microenvironment are in an ideal arrangement for the control of cell functions such as differentiation. For example, in bone tissue, ECM consists of an interwoven fiber network of collagen and elastin including proteoglycans and inorganic hydroxyapatite content.[109] During osteogenesis, cells differentiate into osteoblasts which are the primary cells responsible for bone matrix minerilization by secreting type I collagen and hydroxyapaptite. As these components are secreted into the bone ECM by osteoblasts, matrix porosity and permeability of the mineralized bone tissue as well as growth factor levels decrease. Along with these changes, within the mineralized matrix osteoclastic activity becomes predominant and osteoclasts provide destruction of bone and reabsorbtion of minerals.[110] As such, regulation

of cell functions and reorganization within the tissues are critically linked to not only adhesive and mechanical properties of ECM but also its permeability and porosity.

1.4. HYDROGELS AS ECM MIMICS

Hydrogels are versatile biomaterial platforms for developing ECM analogs for *in vitro* and *in vivo* cell culture and tissue engineering applications. They are ideal candidates for mimics of the native ECM with their high water content, facile transport of oxygen, nutrients and wastes, and tissue-like elasticity.[111] Furthermore, many hydrogels can be formed under mild and cytocompatible conditions, and easily modified with chemical functionalities, mechanical properties and degradability.[112]

Hydrogels can be synthesized from either naturally or synthetically derived polymer systems offering a broad spectrum of chemical and mechanical properties. Naturally derived hydrogels are typically formed of ECM components including collagen[113], hyaluronic acid[114], fibrin[115], dextran[116], and Matrigel[117]. Since, these hydrogels are derived from natural sources, they are inherently bioactive, biocompatible and biodegradable. They also promote cellular functions due to the numerous endogenous factors presented. However, these materials are very complex and it is challenging to determine the isolated effects of single cues on cellular behaviour.[118] In addition, there is risk of contamination, and batch-to-batch variability, which can result in different effects on cells, and make tuning of the biochemical and mechanical properties difficult.

On the other hand, synthetic polymers which provide certainty for the exact composition, biochemical and mechanical properties of the cellular microenvironment have evolved as an attractive platform to investigate the effects of specific biochemical and biophysical signals on cellular behaviour. Many different polymeric building blocks including polyethylene glycol (PEG)[119], poly(vinyl alcohol) (PVA)[120], and poly(2-hydroxy ethyl methacrylate)[121] can be used to form synthetic hydrogels as 2D and 3D cell culture platforms. PEG is considered as a golden standard with its bioinert nature and high hydrophilicity. PEG hydrogels are accepted as a blank state since they lack functional sites to interact directly with cells. Even though, they don't provide any integrin mediated cell material contact, it has been shown that PEG hydrogels support the viability of cells and allow ECM deposition as they are degraded.[122] In addition, the hydroxyl end groups of PEG can be easily modified with other chemical groups such as arylates, metacrylates, maleimides, thiols and azides that can react with each other to form 3D hydrogel networks.[119] These inert hydrogels are highly reproducible with their easy manufacturing process and they allow for precise control over the mechanical properties. However, they lack bioactivity to promote cell behaviour, and act just as a template to permit cellular function.[118] However, some of its biochemical and biophysical cues can be integrated into these convenient hydrogel platforms to properly mimic the complex system of native ECM and bioactive matrices with controllable properties can be obtained.

1.4.1. Bioengineering approaches to create synthetic ECM analogues

The rapid increase in the understanding of matrix biology has provided strategies to utilize the native ECM as an ultimate model for creating functional biomimetic scaffolds.[123] However, understanding the signals that guide cell fate lies at the interfaces of biology, chemisty and materials science. One should consider the biochemical, mechanical and physical properties of the natural cell microenvironment for succesful fabrication of functional tissue analogues.

1.4.1.1. ECM-mimetic bioactive modification

Cell arctitecture and function are affected by the binding of specific ligands to cell surface receptors activating specific signal transduction pathways. Modulation of biological outcomes of the interaction between a biomaterial and cells can be acquired by introducing bioactive molecules that provide signals to direct cellular behaviour.[124] ECM-derived short peptides[125] as well as ECM-derived proteins[126-127] have been intensively used to modify PEG hydrogels to provide chemical cues that modulate cell adhesion, migration, proliferation and differentiation. Usage of the entire protein structure for incorporation of bioactivity can result in the denaturation and degredation of proteins quickly after immobilization. ECM-derived short peptide sequences have the advantage of stability, easy tunability of functions just by changing the amino acid sequences and synthesis in a large scale.[128] Many bioactive short peptide sequences derived from native ECM proteins including collagen, fibronectin and laminin have been utilized to provide biochemical functionality to PEG hydrogels. Current strategies to tether bioactive epitopes to PEG hydrogel networks are mainly based on

covalent attachment via mono-, di-, or multivalent reactive groups such as acrylate, amine, thiol, azide, and maleimide.[123]

Incorporation of bioactive peptide epitopes into the crosslinked polymer matrix induces attachment of cells to the otherwise non-adhesive PEG hydrogels. Cell-adhesive peptide sequences are crucial for regulation of cell-material interactions and cellular functions.[129] RGD is certainly the most widely used short peptide sequence to render PEG hydrogels bioactive.[130-131]

A major approach to create bulk cell-adhesive PEG hydrogels is copolymerization of PEG diacrylate (PEGDA) with monoacrylates of RGD peptide. Hern and Hubbell synthesized monoacrylated RGD monomers with (RGD-PEGMA) or without (RGD-MA) PEG spacers by functionalizing the N-terminal amines of RGD peptides with N-hydroxyl succinimide (NHS) ester of acrylic acid (AA-NHS).[131] Eventually, copolymerization of RGD-MA or RGD-PEGMA monomers with PEGDA resulted in the formation of cell-adhesive photopolymerized PEG matrices. Incorporation of RGD peptide into hydrogel network provided significant increase in fibroblast adhesion and spreading. This method has been studied with various other cell adhesive peptides suchs as YIGSR, REDV, VAPG and IKVAV to incorporate bioactivity into PEG hydrogels.[123]

Another available approach is functionalization of short peptides with the same reactive groups that are employed in the crosslinked polymer network formation. When the functionalized peptides are mixed with polymer precursor solution, the

peptide sequence is distributed within the network upon gelation and can provide signalling to cells.[132] With regard to this strategy, many studies in the literature used acryl-PEG-RGD monomers synthesized by coupling of monoacrylated PEG-*N*-hydroxysuccinimide to the N-terminal α-amino group of the RGD peptide. Along with copolymerization of acryl-PEG-RGD and PEGDA, it is possible to obtain RGD coupled photopolymerized PEG matrices.[131,133] It is shown that, osteoblasts cultured on these hydrogel matrices, presented a higher degree of spreading and cytoskeletal organization. In addition, increase in the mineralization was observed along with increasing RGD epitope concentration.[134]

Another method for peptide coupling to PEG hydrogels is thiol-acrylate photopolymerization. Anseth and co-workers synthesized thiol-containing RGD peptide in the form of CGRGDSG and this peptide was photopolymerized with PEGDA by using UV light for 10 min[135]. This method was cytocompatible for encapsulation of cells within 3D PEG hydrogels to direct cellular functions. Similar to this strategy, Liu et al.[136] functionalized tetrahydroxyl PEG with acrylate and then reacted with thiol-containing RGD peptide. This method was implementad as an injectable PEG/RGD hybrid hydrogel to encapsulate human mesenchymal stem cells (hMSCs) and *in vitro* results confirmed that hMSCs encapsulated within the PEG/RGD hydrogel undergo chondrogenic differentiation with RGD-dose dependence.

Click chemistry has also been employed to fabricate bioactive PEG hydrogels with enhanced mechanical properties. Yang et al. synthesized cell-adhesive PEG

hydrogels by click chemistry between 4-arm PEG acetylene (4-PEG-Ace) and RGD diazide (RGD-2N_3).[137] PEG networks were formed by Copper (I) catalysis between RGD-2N_3 and 4-PEG-Ace forming 1,2,3-triazoles under physiological conditions. Primary human dermal fibroblasts encapsulated into RGD-PEG hydrogels showed significantly improved attachment and proliferation.

These affords provide fundamental knowledge to understand cell-material interactions through cell adhesion. Although these strategies are very straightforward and widely used, several challenges still remain in terms of creating precisely controlled bioactive hydrogels. Incorporation of adhesive peptides into the network requires multistep complex chemical reactions to create functionalized peptide and polymer monomers and the level of peptide incorporation directly influences the network structures and mechanical properties of the resulting covalent network. Therefore, these covalent chemistries are insufficient in terms of offering spatiocontrol over the gel's functionalization.

1.4.1.2. Controlling the mechanical properties

In addition to chemical cues, mechanical properties of materials are also known to influence cell behaviour.[138] Cells generally adhere more strongly to stiffer substrates compared to soft ones.[88] When the cells are attached to surface, they spread out by forming actin-myosin fibers, therefore substrate stiffness influences the cytoskeletal organization and cell morphology. Many studies showed that stiffer substrates support extended cell spreading while the cells on soft substrates

preserve their rounded shape.[139] These changes in cell morphology are accompanied by changes in cell behaviour including differentiation. The effect of substrate stiffness on cellular differentiation was demonstrated by Engler and co-workers.[140] They showed that MSCs commit to a specific lineage with extreme sensitivity to substrate stiffness. It was indicated that soft gels that mimic elasticity of brain tissue are neurogenic, while stiffer matrices that mimic muscle tissue are myogenic, and rigid gels that mimic bone tissue are osteogenic.

The most common way to control the mechanical properties of polymeric materials is by varying the concentarions or molecular weights of polymers and crosslinkers.[141] In one approach, Anseth et al. developed photocrosslinkable gels based on multi-vinyl macromers of PEG and PLA to optimize the compressive modulus of the gel, mimicking the physiological loads.[142] Increasing the initial PEG macromer concentration from 10% to 20% resulted in gels with elastic moduli ranging from 60 to 500 kPa. In another approach, Healy and colleagues developed interpenetrating networks with variable moduli (vmIPN).[143] For the first step of vmIPN synthesis, they polymerized acrylamide gels directly onto the glass surfaces with various amounts of *N*,*N*′-methylenebis(acrylamide) (BIS) to change mechanical stiffness. They used a second layer of $PEG(NH_2)_2$ for the functionalization of surfaces with RGD peptide. They found that soft PEG-peptide based materials with 0.5 kPa moduli mimicking the physiological stiffness of brain promote differentiation of neural stem cell (NMCs) into neurons, while stiff gels with 1-10 kPa moduli promote differentiation into glial cells. Moreover, Gilbert et al. engineered a tunable PEG hydrogel platform by

using PEG-SH and PEG-VS precursors and they produced hydrogels with a range of rigidity by changing the percentage of PEG polymer in the precursor solution.[144] Eventually, skeletal muscle stem cells (MuSCs) on soft PEG hydrogels that mimic muscle elasticity (12 kPa) showed self-renewal and regenerated functional muscle tissue when implanted, while the ones cultured on rigid substrates lost their ability of regeneration.

In summary, current investigations demonstrate that mechanical properties of materials affect cellular behaviour including differentiaton and the cytoskeletal regulation plays an important role in translating feedback from substrate stiffness into cell behaviour.[145] However, all these strategies demonstrate a uni-functional perspective. Further research is still need to investigate the effects of mechanical properties in combination with other factor such as varied bioactive signals and scaffold nanostructure (i.e. porosity, dimensionality) similar to complex microenvironment of native ECM.

1.4.1.3. Tuning the porosity and permeability

Most important concern about the synthetic polymer scaffolds in case of three-dimensional (3D) cell culture is the fact that cells may suffer from lack of nutrients and gases within the 3D matrix. 3D matrices have physical obstacles that prevent cell proliferation, migration and morphogenesis.[141] In general, chemically crosslinked polymer hydrogels form mesh-like structures with pores less than 10 nm. Eventough they provide diffusion, encapsulation of cells within the polymeric matrices prevents cellular events such as spreading, where cells

entrapped within the crosslinked scaffold remain in the rounded morphology and cell functions are restricted.[146]

Researchers have managed to improve diffusion and increase cell functions through different engineering strategies. Some physical techniques such as leaching and gas foaming have been developed to create porous PEG hydrogels. By using crystal colloids that could be further removed by solvent extraction (leaching), PEG scaffolds with pore sizes ranged between 20-60 μm were formed.[147] Another approach, using CO_2 as a porogen, resulted in the formation of pores ranging in size from 100 to 600 μm and MSCs encapsulated into these PEG scaffolds showed enhanced osteogenesis.[148] One recent study indicated that incorporating hydrophilic nanoparticles partially reduced the crosslinking density and improved the permeability of PEG hydrogels and viability as well as functionality of encapsulated cells was improved by this method.[149]

These methods provide cell functionality, transport of nutrient and removal of wastes for cell survival, however, they only allow cell seeding after fabrication process due to non-physiological fabrication conditions and it is hard to control material integrity and mechanical properties by using these strategies.

1.4.1.4. Self assembly as a strategy for structural and bioactive ECM mimics

Self-assembly is the spontenous arrangement of individual building blocks into ordered and stable architectures by means of non-covalent bonds such as hydrogen bonding as well as electrostatic and hydrophobic interactions.[150] The

most commonly investigated self-assembling material for tissue engineering applications is the peptide amphiphile (PA), which contains a hydrophilic peptide region capable of making hydrogen bonds to form β-sheet structure and a hydrophobic region usually consist of a single carbon tail (Figure 1.2. A).[151] Peptide amphiphiles are known to self-assemble into one-dimensional (1D) nanostructures under physiological conditions, forming predominantly nanofibers with a cylindrical geometry (Figure 1.2. B,C,D).[152] The amphiphilic peptides can form hydrogels under physiological conditions by encapsulating water. These fibrous structures closely mimic the features of native ECM with their nanofibrillar architecture and high water content.[153] Furthermore, the resulting nanostructures can be highly bioactive and are of great interest in biomedical applications. Bioactive signalling epitopes derived from native ECM proteins can be easily incorporated into the peptide structure by simply changing the amino acid sequences.[152] However, the nature of non-covalent assembly limits flexibility in terms of tuning the mechanical properties of the resulting PA hydrogels.[154] Therefore, by using the strategies to extend the horizons of self-assembly and integrating these with bioactive manipulation and architectural features, self-assembly can be used to open an entire new chapter in the field of biomimetic scaffold design.

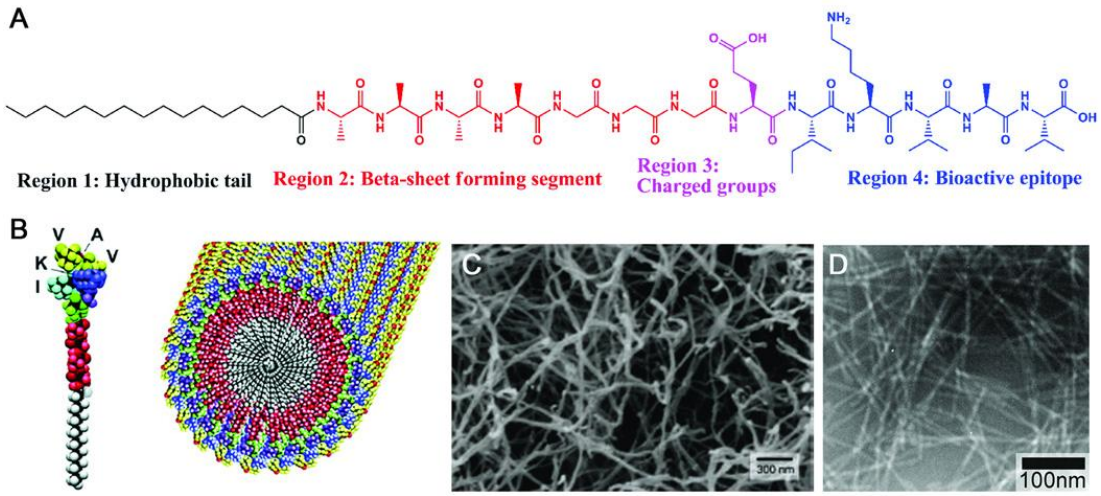

Figure 1.2. A) Molecular structure of a representative peptide amphiphile. B) Molecular graphics illustration of a PA molecule with a bioactive epitope and its self-assembly into nanofibers. C) Scanning electron micrograph of the PA nanofiber network formed by adding cell media (DMEM) to the PA aqueous solution. D). Transmission electron micrograph of the PA nanofibers. (Reproduced with permission from ref. 152, copyright © 2010 John Wiley & Sons, Inc.).

CHAPTER 2

BIOACTIVE POROUS PEG-PEPTIDE COMPOSITE HYDROGELS WITH TUNABLE MECHANICAL PROPERTIES

CHAPTER 2

BIOACTIVE POROUS PEG-PEPTIDE COMPOSITE HYDROGELS WITH TUNABLE MECHANICAL PROPERTIES

2.1 INTRODUCTION

Hydrogels have been intensively studied as molecularly engineered scaffolds for controlled drug delivery[155], cell encapsulation[156] and tissue regeneration[157] applications. They mimic native extracellular matrix (ECM) in terms of its highly hydrated and porous network structure.[112,158-159] However, when the complexity of natural ECM[160] is considered, hydrophilicity and porosity are not sufficient by themselves to meet the design requirements for guiding cellular behavior. The biological outcomes of introducing a biomaterial to the cellular microenvirenment are dependent on cell-material interactions at the nanoscale level.[161] Cells sense their microenvironment with receptors called integrins.[162] They can sense biochemical properties of a material such as the presence of bioactive ligands[130] as well as biophysical characteristics including dimensionality[163] and matrix stiffness[95]. Along with integrin signalling, specific signal transduction mechanisms can be activated within the cells in response to different stimuli and the signalling pathways can regulate cell fate.[66,162,164-166] Therefore, functionalization of hydrogels is crucial for the modulation of cellular characteristics, and plays an important role at biochemical and biophysical interfaces depending on the desired cellular outcome for a specific therapeutic application.

Synthetic polymers have been used as a tool for the modification of biophysical characteristics since they provide convenient control over the mechanical properties.[167] Cells can sense the mechanical properties of their environment and as a response to perceived mechanical stimuli, they generate biochemical activity along with the signal tranduction mechanism called mechanotransduction.[89-90] Matrix stiffness can regulate cellular functions including adhesion[91], spreading[92], migration[93], proliferation[94] and differentiation[95-96]. One of the most commonly used synthetic polymers to investigate the effects of mechanical stimuli on cellular behavior is polyethylene glycol (PEG), which provides precise control over material stiffness. PEG is an ideal hydrogel material with its good water solubility, biocompatibility, nonimmunogenity and resistance to protein adsorption.[168] However, due to its protein-repellent property, PEG alone can not provide cell attachment and induce further cell-material interactions. Current strategies for creating functional PEG hydrogels that provide specific biochemical characteristics of native ECM, require incorporation of ECM-derived bioactive molecules via crosslinking chemistries.[123,169] Short peptide sequences are major targets for addition of bioactivity. Fibronectin derived RGD is the most commonly used adhesive peptide sequence to introduce bioactivity to PEG hydrogels.[123] Various strategies have been described in the literature to create RGD-coupled hydrogel networks of PEG macromers. Micheal-type addition reactions and acrylate polymerization are the most widely utilized crosslinking chemistries.[131,170] Nevertheless, covalent conjugation of functional epitopes to the polymer chain requires complex chemical reactions and can result in limited mobility and accessibility of bioactive ligands.[96] For example, peptide monoacrylates such as RGD-PEGMA (polyethylene glycol monacrylate) can

copolymerize with polyethylene glycol diacrylate (PEGDA) to create cell-adhesive PEG hydrogels with acrylate polymerization.[131] However, due to the indiscriminate polymerization of modified peptide and polymer monomers, the distribution of RGD epitopes within the resulting network is random. Also, peptide incorporation into the hydrogels is limited because the acrylation of peptides affects hydrogel formation and its mechanical properties. Since, ligand presentation and convenient control over the mechanical properties play important role in controlling cell behaviour, crosslinking-chemistries stay as insufficient approaches for incorporation of bioactivity to PEG hydrogels. In addition, limited porosity of the crosslinked PEG hydrogels could prevent cell motility, cell-cell interactions and diffusion, especially in case of three dimensional (3D) culture conditions. A number of approaches have been shown to generate porous PEG networks such as salt leaching[171] and gas foaming[172]. However, these methods require multiple steps and they still have broad pore size distributions reaching up to 600 μm with poor pore interconnectivity. Therefore these strategies are far from presenting a bioactive nanoscale architecture for mimicking the real ECM environment.

When compared to current PEG systems, supramolecular peptide networks which have fibrous structure and tailorable bioactive properties, are versatile hydrogel platforms that can eliminate the limitations of covalent crosslinking.[173-174] Under physiological conditions, supramolecular peptides can self-assemble into one-dimensional nanostructures, predominantly cylindrical nanofibers.[152] Through incorporation of specific amino acids into the sequence, self-assembled peptide networks allow construction of bioactive hydrogels closely imitating the nanoscale

architecture and function of native ECM.[175] The resulting hydrogels can present a variety of bioactive signals on the nanofiber surfaces at high concentration without any limitation of ligand presentation. Current strategies for incorporation of biochemical factors to direct cellular processes, are mainly based on utilization of short peptide sequences derived from the native ECM proteins such as fibronectin[176-177], laminin[178], collagen[179] etc. For instance, previously mentioned RGD epitope has been widely used to produce adhesive self-assembled peptide networks.[176,180-181] It has been shown in many studies that $\alpha_v\beta_1$ integrin binding RGD sequence induce adhesion, spreading and migration of fibroblasts[182], osteoblasts[134] and mesenchymal stem cells[183]. Another bioactive epitope of interest is $\alpha_2\beta_1$ integrin binding DGEA (Asp-Gly-Glu-Ala) derived from collagen type-1. The DGEA peptide can promote survival and osteogenic differentiation of hMSCs and mouse pre-osteoblast MC3T3 cells.[184-186] Self-assembled peptides can be modified to perform a desired function by simply changing the amino acid sequence. Therefore, non-covalently assembled peptide nanofibers can be utilized as versatile ECM mimicking nanostructures displaying a variety of biologically active signals without the need of complex covalent chemistries.

In this work, we present a novel PEG-peptide nanofiber composite hydrogel system with independently tunable biochemical, mechanical and physical cues that does not require any chemical modification of polymer backbone to create synthetic ECM analogues. This approach allows non-interacting modification of multifactorial niche properties (i.e. bioactive ligands, stiffness, porosity), since no covalent conjugation method was used to modify PEG monomers for

incorporation of bioactivity and porosity. Combining the self-assembled peptide nanofibers with crosslinked polymer network simply by facile mixing followed by photo-polymerization resulted in formation of porous hydrogel systems. Resulting porous network can be functionalized with desired bioactive signalling epitopes by simply altering the amino acid sequence of peptide amphiphile molecules. In addition, the mechanical properties of the composite system can be precisely controlled by changing the PEG concentration. Ultimately, multifunctional PEG-peptide composite scaffolds reported in this work, can fill a critical gap in the available biomaterials as versatile synthetic mimics of ECM with independently tunable properties. Such a system could provide a useful tool allowing the investigation of how complex niche cues interplay to influence cellular behaviour and tissue formation both in 2D and 3D platforms.

2.2 MATERIALS & METHODS

2.2.1. Materials

All protected amino acids, lauric acid, Rink amide MBHA resin, Fmoc-Glu(OtBu)-Wang resin (100-200 mesh), Fmoc-Aps(OtBu)-Wang resin (100-200 mesh), *N*,*N*,*N*′,*N*′-Tetramethyl-O-(1*H*-benzotriazole-1-yl) uranium hexafluorophosphate (HBTU) and diisopropylethylamine (DIEA) were purchased from Novabiochem ABCR or Sigma-Aldrich. All other chemicals and materials used in this study were analytical grade and purchased from Invitrogen, Fisher, Merch, Alfa Aesar, and/or Sigma-Aldrich.

2.2.2. Synthesis and Characterization of Peptide Amphiphiles

Fmoc solid phase peptide synthesis method was employed to synthesize Lauryl-Val-Val-Ala-Gly-Lys-Lys-Lys-Am (K_3-PA), Lauryl-Val-Val-Ala-Gly-Glu-Glu-Glu (E_3-PA), Lauryl-Val-Val-Ala-Gly-Glu-Arg-Asp (RGD-PA), Lauryl-Val-Val-Ala-Gly-Glu-Gly-Asp-Gly-Glu-Ala-Am (DGEA-PA). For K_3-PA and DGEA-PA Rink amide MBHA resin (Novabiochem) served as the solid support while Fmoc-Glu(OtBu)-Wang resin (100-200 mesh) and Fmoc-Asp(OtBu)-Wang resin (100-200 mesh) were used for E_3-PA and RGD-PA as solid supports. Carboxylate group activation of 2 mole equivalents of amino acid was succeeded by 1.95 mole equivalents of HBTU, and 3 mole equivalents of DIEA for 1 mole equivalent of functional sites on the solid resin. Fmoc groups were removed at each coupling step with 20% piperidine/dimethylformamide for 20 min. Amino acid coupling time was set to be 2 h at each cycle. Lauric acid served as the source of lauryl group and its coupling mechanism was similar to amino acid coupling. 10%

acetic anhydride-DMF solution was used to permenantly acetylate the unreacted amine groups after each coupling step. Cleavage of protecting groups and peptide molecules from the solid support was carried out by trifluoroacetic acid (TFA) cleavage cocktail (95% TFA, 2.5% water, 2.5% triisopropylsilane) for 3 h. Excess TFA was removed by rotary evaporation. Synthesized peptides were then precipitated in diethyl ether overnight. The precipitate was collected by centrifugation and dissolved in ultra pure water. This solution was frozen at -80 °C followed by lyophilization for one week. The purity of the peptides was assessed using Agilent 6530 quadrupole time of flight (Q-TOF) mass spectrometry with electrospray ionization (ESI) source equipped with reverse-phase analytical high performance liquid chromatography (HPLC). Syntesized peptides were purified with a preparative HPLC system (Agilent 1200 series). All peptide molecules were freeze-dried and reconstituted in ultrapure water at pH 7.4 before use.

2.2.3. Transmission Electron Microscopy (TEM) Imaging of PA Nanofibers

For TEM imaging the samples were prepared by mixing 1 mM PA solutions at 3:4 (E_3-PA/K_3-PA), 3:2 (RGD-PA/ K_3-PA), and 1:1 (DGEA-PA/K_3-PA) ratios on a 200 mesh carbon TEM grid. After 5 min incubation, the unbound peptide nanofibers were rinsed off with water and the remaining peptide nanofibers were air-dried in a fume hood. Staining was performed with uranyl acetate. TEM imaging was performed with a FEI Tecnai G2 F30 transmission electron microscope at 300 kV.

2.2.4. Preperation of 2D Hydrogels

Poly (ethylene glycol) dimethacrylate (PEGDMA) (Mn=550, Aldrich) was dissolved in ultra pure water (pH 7.4) at different concentrations, 4%, 8% and 12% (w/v). A photoinitiator, 2,2'-Azobis(2-methyl-propionamidine)dihydro-chloride) (Aldrich) (1.0 w/v) in ultra pure water was dissolved and added to the PEGDMA solution at a final concentration of 0.1% (w/v). Synthesized peptides were dissolved in ultra pure water (3% w/v) and added to PEGDMA-photoinitiator solution one by one with a final concentration of 1.5% (w/v) in case of PEG-peptide composite hydrogels. Oppositely charged peptide combinations were used in sufficient volumetric ratios to trigger nanofiber self-assembly through charge neutralization. Peptide combinations were determined as E_3-PA+K_3-PA (3:4), RGD-PA+K_3-PA (3:2), DGEA-PA+K_3-PA (1:1). Pre-gel solutions were exposed to ultraviolet (UV) light at 365 nm wavelength for 15 min in cell culture plates (48 well-plate or 96 well-plate) for the formation of crosslinked 2D hydrogel substrates.

2.2.5. Preparation of 3D Hydrogels

Similar simple preperation approach was applied to encapsulate Saos-2 cells into 3D matrices. Only difference was that all peptide and PEG-photoinitiator solutions were prepared with Dulbecco's Modified Essential Medium (DMEM) instead of water and cell suspension ($1x10^6$ cells/sample) was mixed with PEG-photoinitiator solution before the addition of PA solutions into the mixture. Total volume of the pre-gel solutions was 200 µl. After the preperation of pre-gel solutions, mixtures were transferred into the caps of eppendorf tubes and exposed

to UV light at 365 nm for 15 min. The resulting disc-shaped 3D gels containing encapsulated Saos-2 cells were cultured in Synthecon RCCS-4H bioreactor system.

2.2.6. Scanning Electron Microscopy (SEM)

To visualize the resulting network formation within the polymerized samples scanning electron microscopy (SEM) was employed. SEM samples were prepared on cleaned silicon wafer surfaces with a similar approach to preperation of 2D hydrogels. Following the UV crosslinking, samples were dehydrated in gradually increasing concentrations of ethanol solutions. The dehydrated hydrogels were dried with a Tourismis Autosamdri-815B critical-point-drier to preserve the network structures. A FEI Quanta 200 FEG scanning electron microscope with an ETD detector was used for visualization of resulting Networks. Samples were sputter coated with 4 nm gold/palladium prior to imaging.

2.2.7. Oscillatory Rheology

An Anton Paar Physica RM301 Rheometer with a 25 mm paralel-plate configuration was used to characterize viscoelastic properties of PEG, peptide and PEG-peptide hydrogels. Crosslinked PEG and PEG-peptide gels were formed inside 48-well cell culte plates and then transferred on the lower plate of the rheometer while peptide gels were formed *in situ* on the rheometer plate. Total volume of the samples was 300 µl and shear gap distance was 500 nm. All measurements were carried out at room temperature. Gelation kinetics of the gels was characterized with time-dependent rheology. During the time-sweep test,

angular frequency and strain were held constant at 10 rad s^{-1} and 0.01% respectively. To determine the linear viscoelastic range (LVR) of the gels, amplitude sweep test was conducted at constant angular frequency of 10 rad s^{-1} with logarithmically ramping the strain amplitude from 0.01 to 1000%.

2.2.8. Brunauer-Emmett-Teller (BET) Analysis

Pore size distribution, total pore volume and specific surface area of PEG and PEG-peptide samples were estimated by using BET analysis. Before the analysis samples were dehydrated in gradually increasing concentrations of ethanol solutions. Dehydrated samples were dried with a Tourismis Autosamdri-815B critical-point-drier to prevent the shrinkage and to preserve the network structures. Samples were degassed at 150 ˚C for 4 h and N_2 adsorption was conducted at 77 K. Total pore volume and specific surface area of the samples were calculated by using quenched solid density functional theory (QSDFT).

2.2.9. Cell Culture and Maintenance

Saos-2 human osteosarcoma cells (ATCC®HTB-85™) were used in adhesion, spreading, viability, immunocytochemistry and gene expression experiments. All cells were cultured in 75 cm^2 cell culture flasks using Dulbecco's Modified Eagle Medium (DMEM) supplemented with 10% Fetal Bovine Serum (FBS), 1% penicilin/streptomycin and 2 mM L-glutamine. Cells were kept at 37 °C in a humidified chamber supplied with 5% CO_2. All *in vitro* experiments and passaging were carried out at cell confluency between 80 to 90% using trypsin/EDTA chemistry. The culture medium was changed every 3–4 days. For

osteogenic differentiation experiments (ICC stainings, qRT-PCR analysis), cell medium was replaced with osteogenic medium, DMEM supplemented with 10% FBS, 10 mM β-glycerophosphate, 50 μg ml^{-1} ascorbic acid and 10 nM dexamethasone, after reaching confluency.

2.2.10. Viability of Saos-2 Cells on PEG and PEG-peptide Substrates

Viability of Saos-2 cells were analyzed on PEG and PEG-peptide substrates prepared in 48 well cell culture plates. Tissue culture plate surface were also used to evaluate the viability of the cells on a control sample. Prior to cell seeding, crosslinked substrates were washed with 1X Phosphate Buffered Saline (PBS) overnight. Cells were seeded onto hydrogel and tissue culture plate surfaces with DMEM media supplemented with 10% FBS, 1% penicilin/streptomycin and 2 mM L-glutamine at density of $1.5x10^4$ cells/cm^2 respectively. After 3 days of incubation, the cell medium was discarded, the cells were washed with PBS and then incubated with 2 μM Calcein-AM/Ethidium homodimer (Invitrogen) in PBS for 20–30 min at room temperature. Finally, random images were taken at 10× magnification from each well for qualitative analysis by fluorescence microscopy.

2.2.11. Adhesion of Saos-2 Cells on PEG and PEG-peptide Substrates

To determine the effect of protein-repellent property of PEG on cellular adhesion, adhesion of Saos-2 cells were analyzed on PEG and PEG-peptide hydrogels prepared in 48-well cell culture plates. Cells were seeded on hydrogel surfaces at density of $1.5x10^4$ cells/cm^2 in serum-free culture conditions with DMEM media supplemented with 1% penicilin/streptomycin and 2 mM L-glutamine. The cells

were incubated at standart cell culture conditions. After 24, 48 and 72 h the unbound cells were washed away three times with PBS, and the remaining bound cells were stained with 2 μM Calcein-AM. Cell adhesions were quantified by counting the number of cells on different locations

2.2.12. Spreading and Cytoskeletal Organization Analysis of Saos-2 Cells on PEG and PEG-peptide Substrates

Spreading and cytoskeletal organization of Saos-2 cells were analyzed on PEG and PEG-peptide surfaces at 72 h. Preparation of the samples was the same as the samples for the adhesion assay. Before staining, cells were fixed with 3.7% formaldehyde for 15 min and permeabilized with 0.1% Triton X-100 for 10 min. Actin filaments of the cells were stained with TRITC-conjugated phalloidin (Invitrogen) in 1X PBS for 20 min. Spreading and cytoskeletal organization of cells were analyzed with Zeiss LSM 510 confocal microscope. Cell spreading was quantified by measuring the spreading areas of cells with Image J program. At least 30 random images were taken per substrate (n=3).

2.2.13. Immunocytochemistry (ICC)

Before ICC stainings, differentiated cells were fixed with 4% formaldehyde for 15 min and permeabilized with 0.5% Triton-X for 10 min at room temperature. 3 wt% BSA/PBS was used for blocking for 1 h. Rabbit-raised, anti-human, RUNX2 and COL1 primary antibodies and a goat-raised, anti-rabbit, IgG H&L DyLight 488 conjugated secondary antibody (Abcam) were used for staining. The samples were visualized with a Zeiss LSM 510 confocal microscope.

2.2.14. Quantitative Reverse Transcription Polymerase Chain Reaction

RUNX2 and COL1 gene expression profiles for osteogenic differentiation were examined by qRT-PCR. Total RNA of differentiated Saos-2 cells was isolated on day 3 and day 7 using TRIzol reagent (Ambion) according to the manufacturer's protocol. Nanodrop 2000 (Thermo Scientific) was used to quantify the yield and purity of the isolated RNA. Primer sequences were designed using Primer 3 software (Table S2). SuperScript III Platinum SYBR Green One-Step qRT-PCR kit was used to carry out qRT-PCR. Temperature cycling for the reaction was determined as 55 °C for 5 min, 95 °C for 5 min, 40 cycles of 95 °C for 15 s, T_m (58.0 °C for RUNX2 and GAPDH, 60.0 °C for COL1) for 30 s, and 40 °C for 1 min. Gene expressions were normalized to GAPDH as the internal control gene.

2.2.15. Statistical Analysis

All experiments were independently repeated at least twice with at least three replica for each experimental group. All quantitative results were expressed as ± standard error of means (s.e.m). Statistical analyses were carried out by one-way or two-way analysis of variance (ANOVA), whichever applicable. For the statistical significance, a *P*-value of less than 0.05 was considered.

2.3. RESULTS & DISCUSSIONS

2.3.1. Peptide Amphiphiles

As mentioned in the materials and methods section, Fmoc solid phase peptide chemistry was employed to synthesize peptide amphiphile (PA) molecules. Four different PA molecules [Lauryl-VVAGEEE (E_3-PA), Lauryl-VVAGERGD (RGD-PA), Lauryl-VVAGEGDGEA-Am (DGEA-PA), Lauryl-VVAGKKK-Am (K_3-PA)] were synthesized (Figure 2.1).

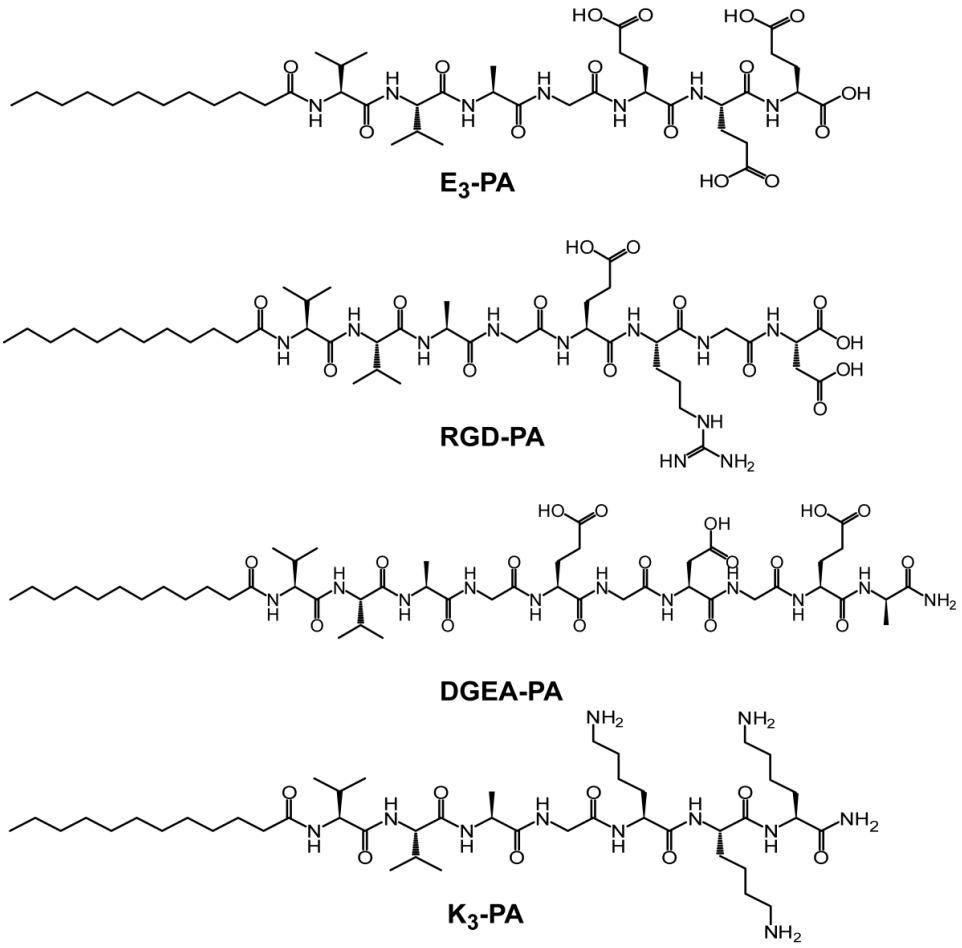

Figure 2.1. Chemical representations of Lauryl-VVAGEEE (E_3-PA), Lauryl-VVAGERGD (RGD-PA), Lauryl-VVAGEGDGEA-Am (DGEA-PA) and Lauryl-VVAGKKK-Am (K_3-PA).

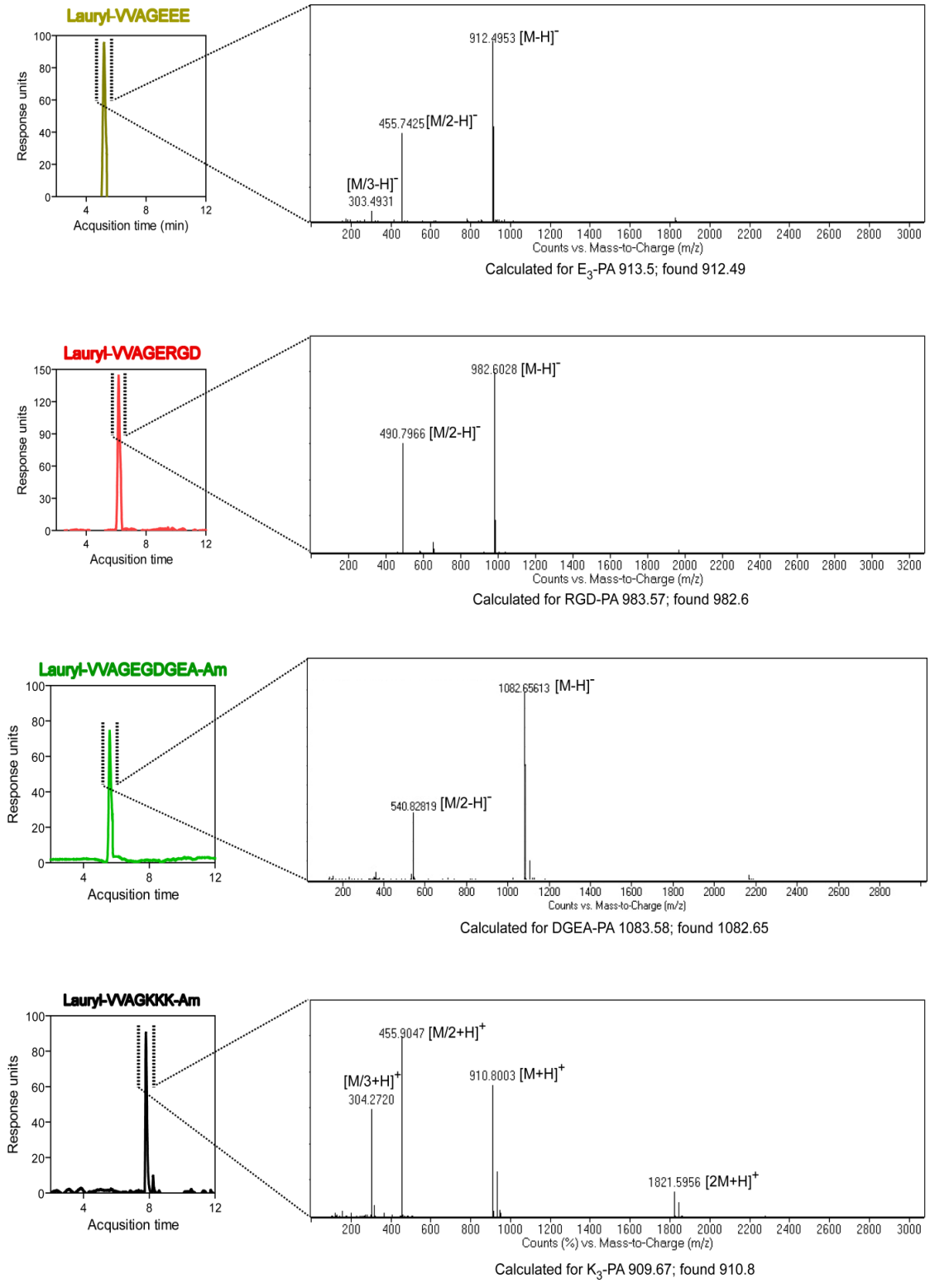

Figure 2.2. Liquid chromatography-mass spectrometry (LC-MS) analysis of the synthesized PAs. The purities of the crude products were analyzed according to the optical density at 220 nm.

After the synthesis, peptides were purified with HPLC and the purity of the peptides was analyzed via LC-MS. As the liquid chromatogram demonstrates, there was only one major product peak, which means only one type of material exists in sample solution. Observed mass spectra ensured the purity of the peptide (Figure 2.2).

2.3.2. Self-assembly of PA Nanofibers

TEM images confirmed the self-assembly of peptide amphiphiles into one dimensional nanofibers. All of the PA combinations resulted in the formation of similar nanostructures (Figure 2.3).

2.3.3. Synthesis of 2D Hydrogels

To synthesize PEG-peptide composites, polyethylene glycol dimethacrylate (PEGDMA, M_n=550) was used because of its biological inertness, cell compatibility and ability to photo-crosslinking. Photo-crosslinking is desirable for biomedical applications with the mild and rapid reaction conditions, which can be conducted at physiological temperature and pH. For the modulation of mechanical stiffness, three different PEG concentrations (4%, 8%, and 12% w/v) were used. E_3-PA was used as non-integrin binding peptide sequence, while RGD-PA and DGEA-PA were exploited as integrin binding epitopes to investigate the effect of different bioactive signals on cellular behaviour. K_3-PA was utilized to induce nanofibrous assembly with its positive net charge when mixed with other negatively charged PA molecules.

To obtain porous hydrogel networks with independently tunable mechanical and

biochemical properties, a very simple fabrication method was implemented. A photoinitiator, 2,2'-Azobis (2-methyl-propionamidine) dihydro-chloride was dissolved in ultra pure water and added into the PEG solution with a final concentration of 0.1% (w/v). Oppositely charged peptide combinations were used in sufficient volumetric ratios to trigger nanofiber self-assembly through charge neutralization at neutral pH. The peptides were dissolved in ultra pure water and added into PEG-photoinitiator solution one by one at a final concentration of 1.5% (w/v) for PEG-peptide composite hydrogels. Net charges of PA molecules, nomenclature of PEG-peptide composite systems, nanofiber compositions and volumetric mixing ratios of PA molecules are shown at Table 2.1 and Table 2.2. The solutions were exposed to ultraviolet (UV) light at 365 nm wavelength for 15 min to induce photo-polymerization. Crosslinking occurred through radical polymerization in which the methacrylate groups participate in an addition reaction to form a branched polymeric network (Figure 2.4).

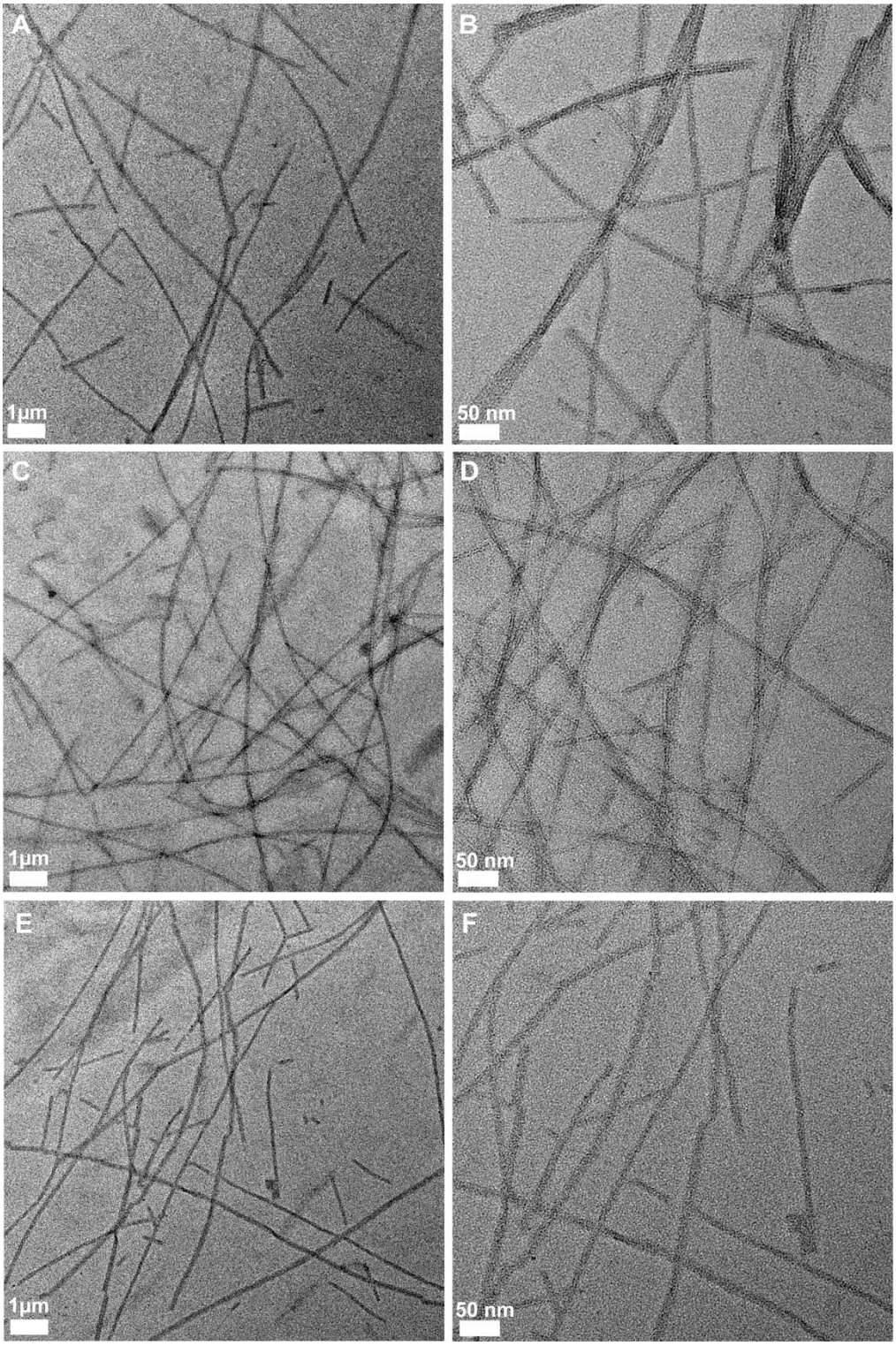

Figure 2.3. Tranmission Electron Microscopy (TEM) images of PA combinations. A), B) E_3-PA/K_3-PA C), D) RGD-PA/ K_3-PA E), F) DGEA-PA/K_3-PA.

Table 2.1. Bioinspired self-assembling PA building blocks.

PA sequence	**Nomenclature**	**Net charge***
Lauryl-VVAGEEE	E_3-PA	-4
Lauryl-VVAGKKK-Am	K_3-PA	+3
Lauryl-VVAGERGD	RGD-PA	-2
Lauryl-VVAGEGDGEA-Am	DGEA-PA	-3

* Theoretical net charge at pH 7.4

Table 2.2. Nomenclature and composition of PEG and PEG-peptide composite hydrogels.

Nomenclature	**Nanofiber composition**	**Mixing ratio**
PEG (w/o peptide)	------	------
E_3-PEG	E_3-PA/K_3-PA	3:4
RGD-PEG	RGD-PA/K_3-PA	3:2
DGEA-PEG	DGEA-PA/K_3-PA	1:1

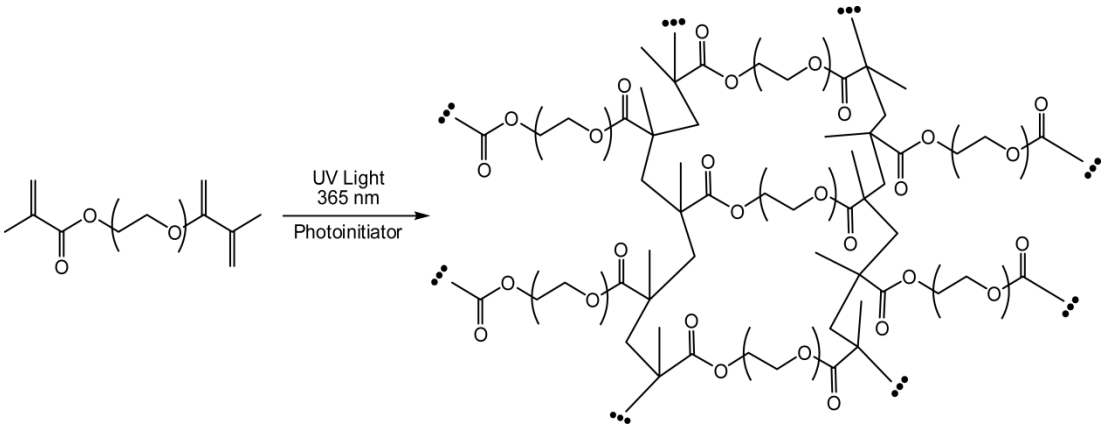

Figure 2.4. Crosslinking mechanism of PEGDMA. Crosslinking occured through radical polymerization in which the methacrylate groups participate in an addition reaction to form a branched polymeric network. Each PEGDMA monomer has two methacrylate groups which can react with up to two other methacrylate groups. Each PEGDMA monomer can covalently link to up to four other PEGDMA monomers and the resulting polymer forms a covalently crosslinked branch.

2.3.4. Material Characterizations

A total of twelve groups were examined as non-bioactive PEG (w/o peptide nanofibers) control versus PEG-peptide composite scaffolds, biochemical cues (E_3-PA as non-integrin binding sequence, RGD-PA & DGEA-PA as integrin binding epitopes in Figure 1A), and mechanical stiffness (PEGDMA concentrations 4%, 8%, and 12% wt defined as soft, medium and stiff in Figure 2.9).

2.3.4.1. Scanning Electron Microscopy (SEM) Imaging of Resulting Networks

Scanning electron microscopy (SEM) was used to visualize the resulting networks. SEM images revealed that the incorporation of non-covalently assembled peptide nanofibers within the crosslinked PEG network resulted in

formation of fibrous porous scaffolds, while the PEG (w/o peptide nanofibers) control was observed as a flat surface. The morphology of the porous networks was similar for all of the groups with different PEG concentrations and peptide combinations (Figure 2.5).

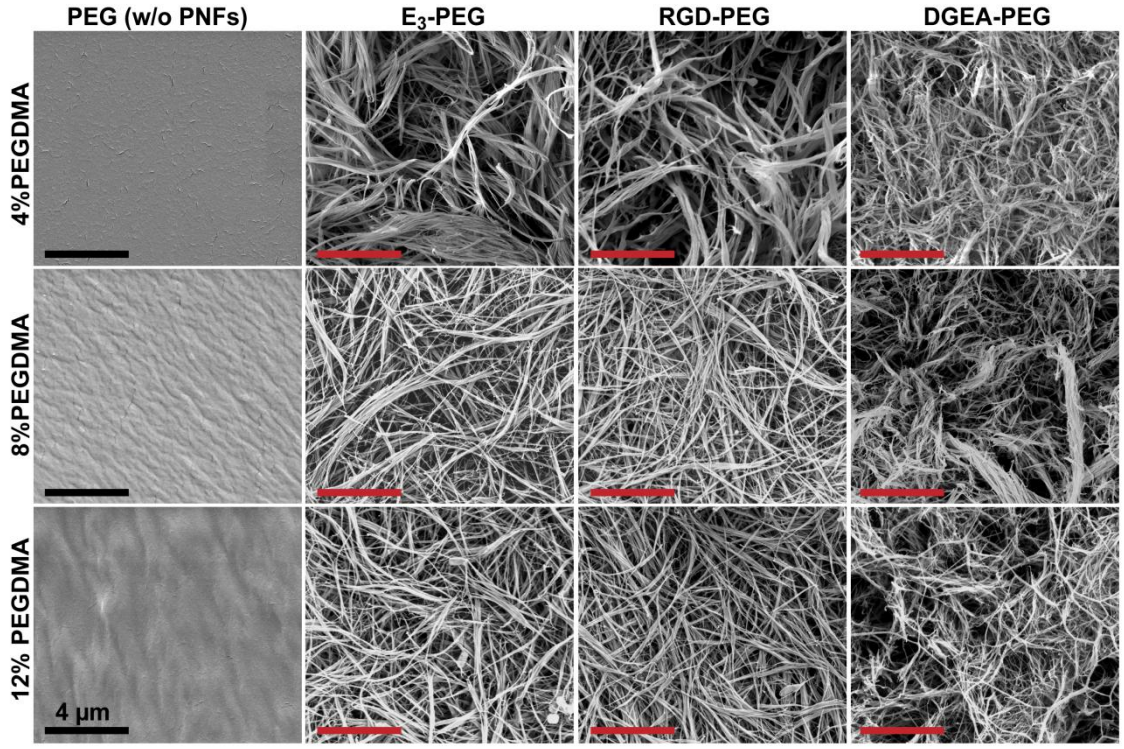

Figure 2.5. Scanning electron microscopy (SEM) images of PEG (w/o peptide nanofibers) and PEG-peptide composites.

2.3.4.2. Porosity and Surface Area Analysis with Brunauer-Emmett-Teller (BET) Method

We also quantitatively analyzed the porosity of the resulting networks with BET (Brunauer-Emmett-Teller) analysis. Pore size distribution, cumulative pore volume and specific surface area of the samples were measured after the hydrogels were dried with critical point drier to prevent the shrinkage of the networks. Due to the highest water content of the 4% PEG group, it was not possible to get realistic results after drying, therefore the "soft" hydrogel group was eliminated from this analysis. As seen from the pore size distributions, the resulting networks consist of pores in a range of up to 35 nm in case of the incorporation of peptide nanofibers and also contain several smaller pores (< 5 nm) (Figure 2.6). Such mesoporous structures are beneficial for tissue engineering, since the pores in the nanometer range can support cell adhesion and proliferation and can potentially allow protein and growth factor absorption at the implant site.[187-188] Also, the results showed the increase in total pore volume and specific surface area of the resulting networks up to 4 fold by the incorporation of peptide nanofibers compared to PEG (w/o peptide nanofibers) scaffolds (Figure 2.7). The increase in the total pore volume is also desirable for facilitation of nutrient diffusion and promotion of cell proliferation as well as ECM production.[189]

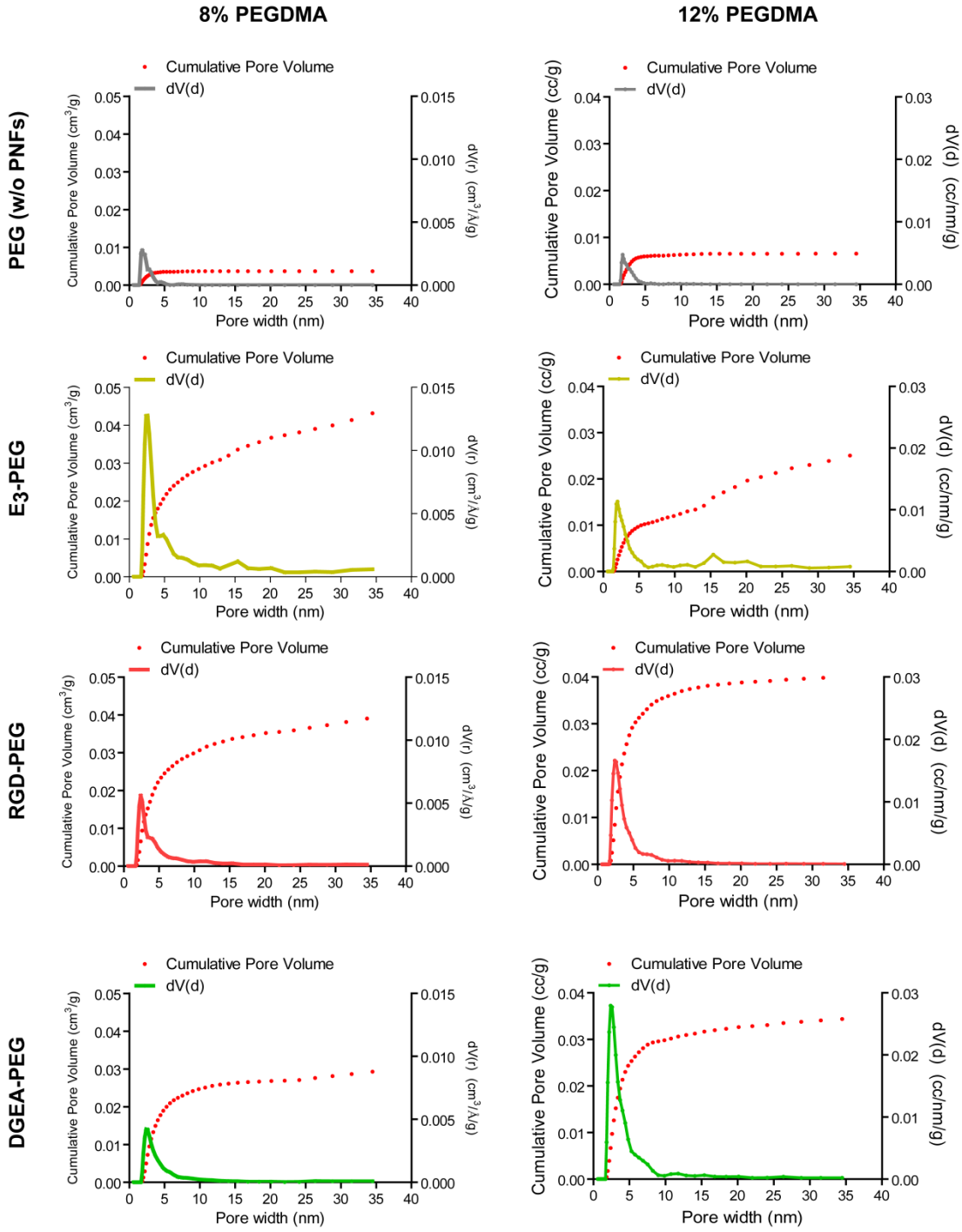

Figure 2.6. BET analysis showing the pore size distributions and cumulative pore volumes of PEG (w/o peptide nanofibers) and PEG-peptide composites.

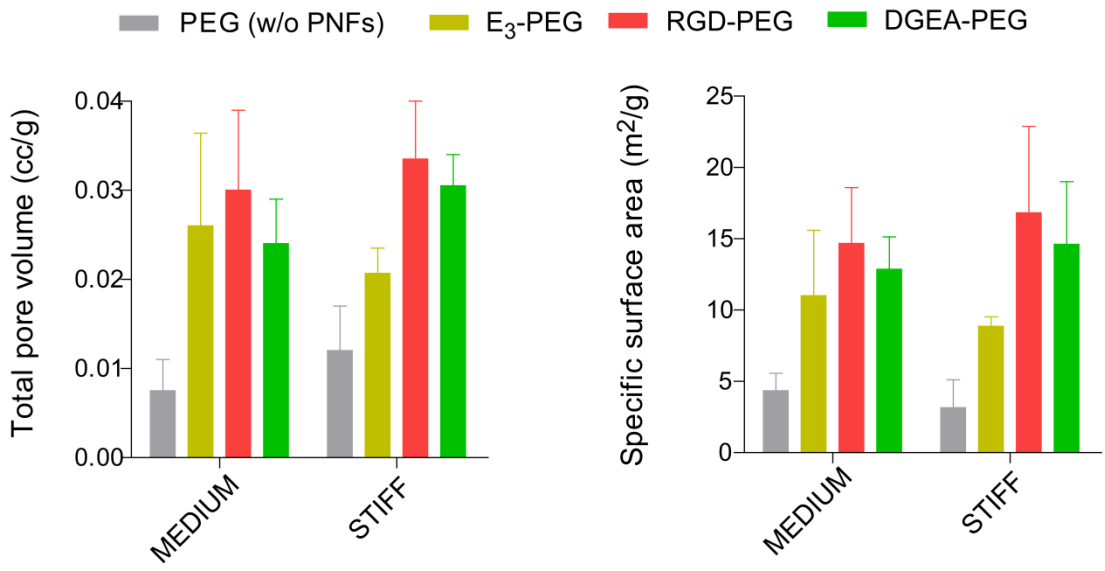

Figure 2.7. Total pore volume and specific surface area of PEG (w/o peptide nanofibers) and PEG-peptide composite scaffolds.

2.3.4.3. Mechanical Characterization–Oscilatory Rheology Analysis

We examined the mechanical properties of the resulting networks. Gelation properties and viscoelastic behaviour of the hydrogels were evaluated with oscilatory rheology.

2.3.4.3.1. Time Sweep Test

Average equilibrium moduli of the gels were determined to assess the mechanical stiffness of the samples as a function of constant angular frecuency (10 rad s^{-1}). For all of the combinations, storage modulus (G'), energy stored during deformation, was greater then loss modulus (G''), energy dissipiated during deformation, confirming the gel character of the resulting networks (Figure 2.8). The mechanical limits of the gels defined as soft, medium and stiff ranged from

0.1-0.3 to 1-4 and 6-8 kPa (Figure 2.9). Consistent increase of the mechanical stiffness for each individual peptide combination along with the increasing PEG concentration revealed the versatility of the composite network for the precise control of mechanical properties.

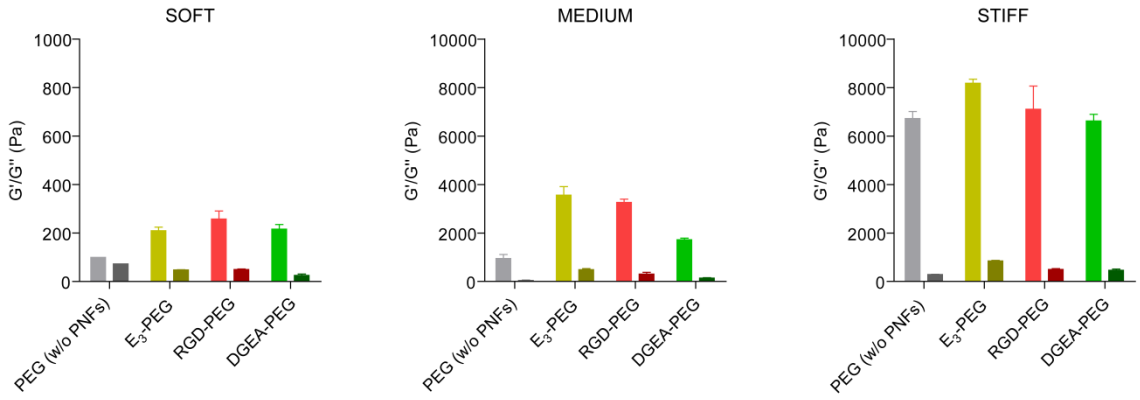

Figure 2.8. Storage/loss moduli of PEG (w/o peptide nanofibers) and PEG-peptide samples showing the gel character of resulting networks.

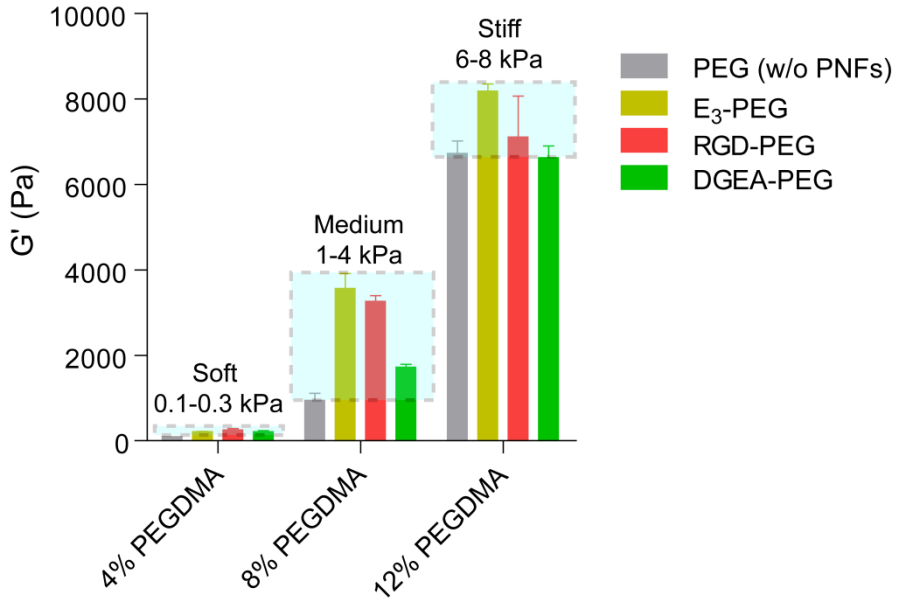

Figure 2.9. Equilibrium storage moduli of PEG (w/o peptide nanofibers) and PEG-peptide composite hydrogels.

2.3.4.3.2. Amplitude Sweep Test

We also performed amplitude sweep test to investigate the viscoelastic properties of the hydrogels. Within a region called linear viscoelastic range (LVR), materials maintained their elastic behaviour by keeping the storage modulus constant under elastic deformation. When the certain boundary of LVR referred as limiting strain amplitude (LSA) was exceeded, plastic deformation occurs and the modulus of the gels starts decreasing under increasing strain values. The length of the LVR can be considered as a measure of stability and gives information about the elasticity of the materials. The results demonstrated that LVR of PEG-peptide composite hydrogels was comparible to PEG (w/o peptide nanofibers) controls while the LVR of the regular supramolecular peptide hydrogels was quite narrow (Figure 2.10A). LSA of individual PEG-peptide groups was similar to each other and reached up to 20% while the LSA of regular peptide hydrogels remained under 0.5% (Figure 2.10B). As in the case of stiff hydrogels, even though the storage moduli of the regular peptide gels (~10 kPa) were similar to PEG-peptide composites, it was not possible to handle only peptide gels like the composite systems due to their low elasticity (Figure 2.11). These results confirmed the increased stability and elasticity of the composite system especially for load bearing tissues such as bone.

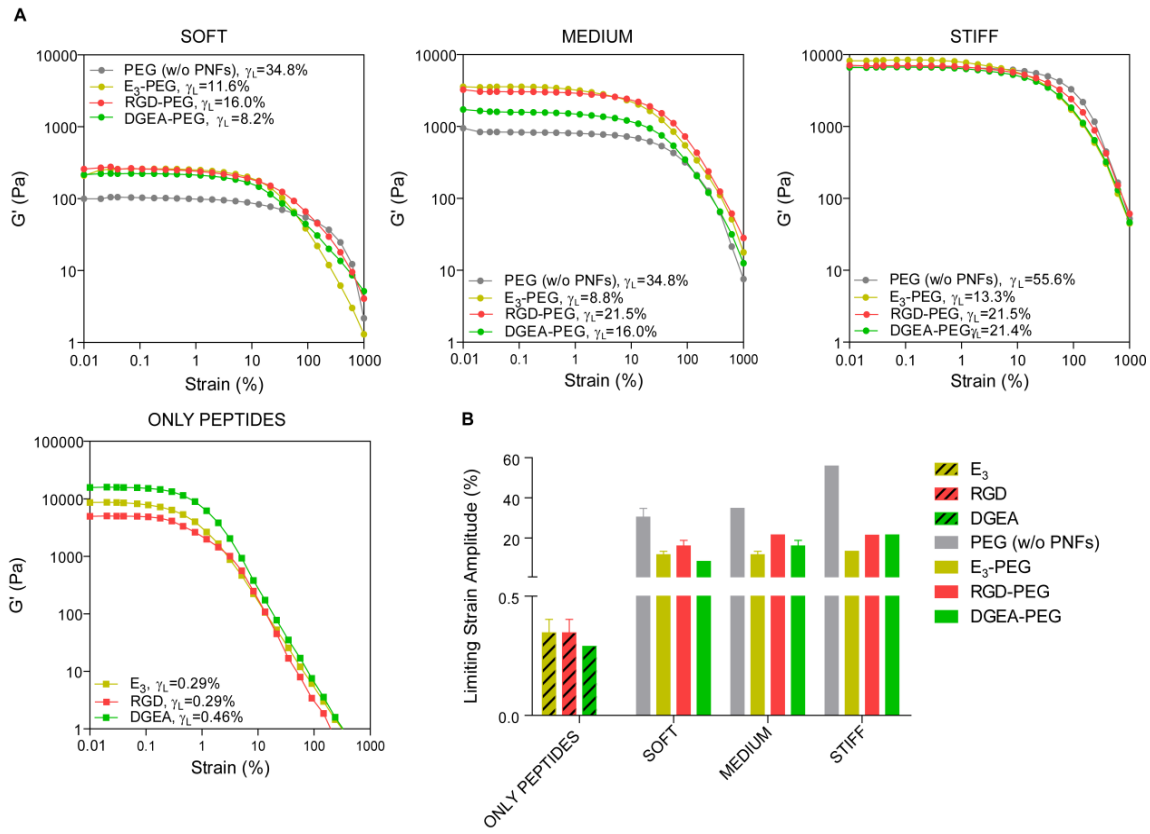

Figure 2.10. Rheological characterizations of gels. A) Amplitude sweep tests and B) limiting strain amplitude values of PEG (w/o peptide nanofibers), PEG-peptide composites and only peptide gels.

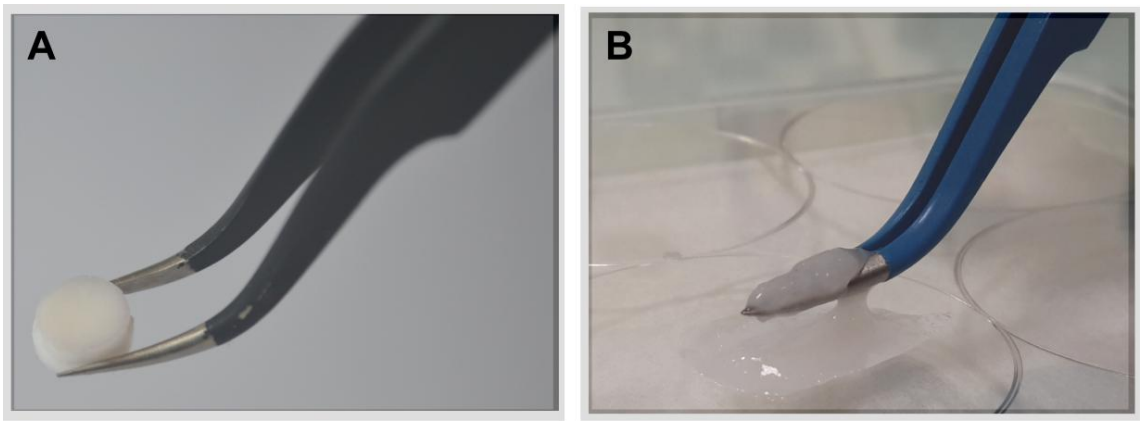

Figure 2.11. Photographs of A) PEG-peptide (E_3-PEG, 12% wt PEGDMA) and B) only peptide gel (E_3+K_3) with the same storage moduli showing the increased elasticity and stability of the composite system.

2.3.5. Investigation of Cellular Behaviour

After the physical and mechanical characterizations, we investigated the cellular behaviour as a response to complex niche cues of the resulting hydrogels. To confirm the biological functionality of the resulting hydrogels and examine the cell response to our multifunctional systems, osteoprogenitor Saos-2 cells were cultured on 2D surfaces. To evaluate the combinational effect of different biochemical signalling epitopes along with the varied mechanical properties, viability, adhesion, spreading and differentiation characteristics of cells were investigated.

2.3.5.1. Live/Dead Assay

First, we examined cytotoxicity and ability to support cell adhesion as a combined function of bioactivity and stiffness. Live/dead assay was performed to determine the toxicity of resulting hydrogels. Live cells were stained with Calcein-AM (green), while the dead ones were stained with ethidium homodimer (red). Both PEG (w/o peptide nanofibers) and PEG-peptide hydrogels were found to be cytocompatible for all combinations. There were only a few dead cells stained as red in the live/dead images (Figure 2.12).

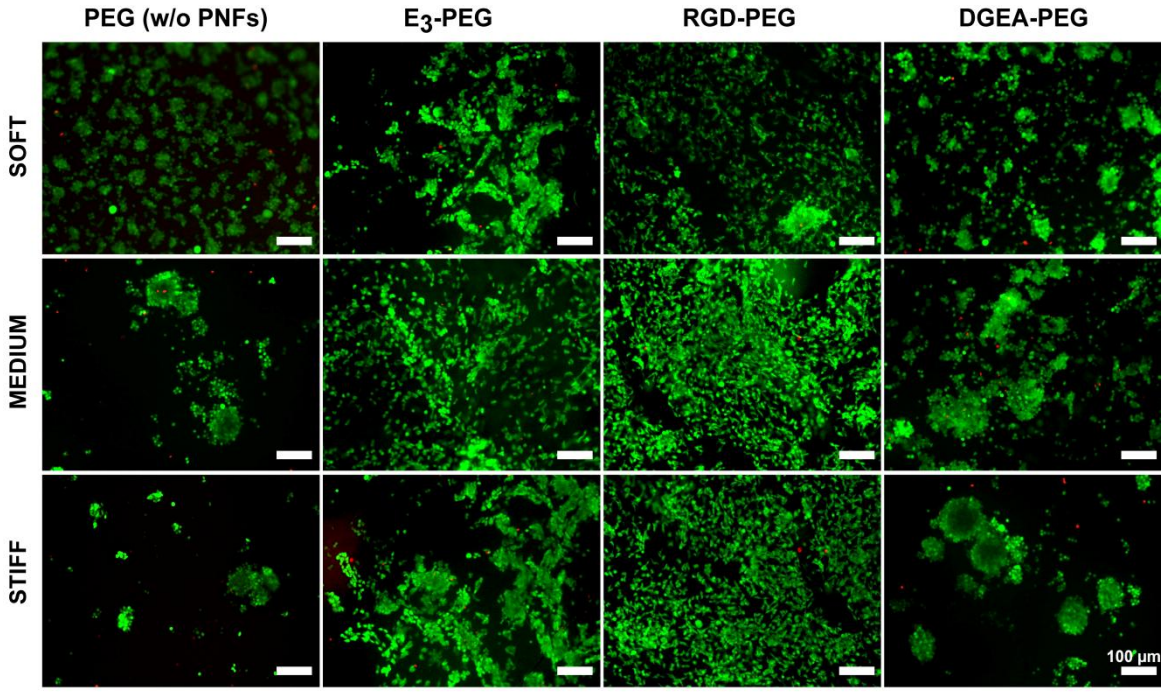

Figure 2.12. Representative Calcein-AM/ethidium homodimer stained micrographs of Saos-2 cells on PEG (w/o peptide nanofibers) samples and PEG-peptide composites showing the non-toxic effect of hydrogel scaffolds. Alive cells were stained with Calcein-AM (green), dead cells were stained with ethidium homodimer (red).

2.3.5.2. Adhesion Assay

Cell adhesion to hydrogel surfaces was examined in serum-free culture conditions. Calcein-AM stainings were performed to evaluate cellular adhesion at the early period of cell culture (24 h). As seen from Calcein-AM stained micrographs, non-bioactive PEG (w/o peptide nanofibers) control was not able to support the cell attachment to the hydrogel surface (Figure 2.13A) at 24 h. It was an expected result since PEG hydrogels are considered as protein-repellent materials which inhibit cell adhesion. On the other hand, PEG-peptide composite

scaffolds supported the adhesion up to 20-30 fold even at the early period of cultivation (24 h) compared to non-bioactive PEG (w/o peptide nanofibers) scaffolds in case of medium and stiff gel combinations. Independent from the availability of integrin binding epitopes, presence of peptide nanofibers within the system was sufficient to promote cell attachment. Non-integrin binding E_3-PEG combination supported the early adhesion at the same level with RGD-PEG and DGEA-PEG combinations (Figure 2.13B). In the case of soft hydrogels, it appeared as PEG (w/o peptide nanofibers) control provides cell attachment closer to PEG-peptide composites according to the quantitave analysis based on the number of attached cells (Figure 2.13B). However, this result was due to the embedding of cells into the soft PEG (w/o peptide nanofibers) hydrogel after seeding. During the staining procedure even after the washing steps cells were not removed from the hydrogel since they were enclosed within the matrix. However, they stayed in the spherical shape without creating any cell-material contact while the ones on composite surfaces created adhesion points as supported by the actin staining results (Figure 2.15A). When the further periods (48 h and 72 h) of cultivation were evaluated, the number of attached cells was drastically increased on PEG-peptide composite system while no increase was observed in the case of PEG (w/o peptide nanofibers) control (Figure 2.14).

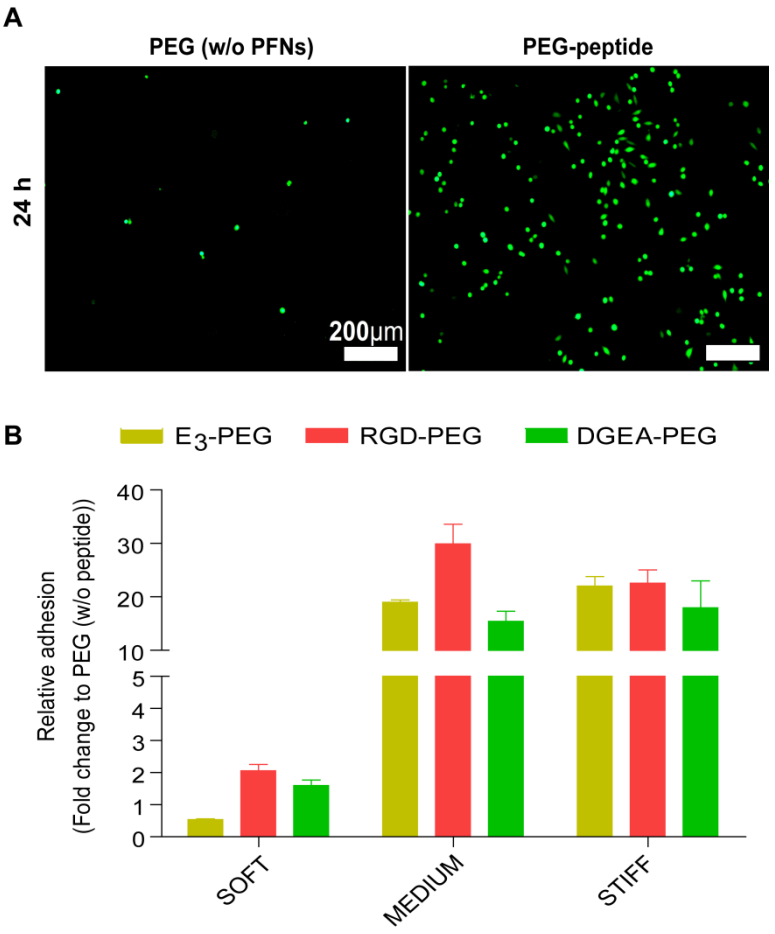

Figure 2.13. A) Representative Calcein-AM stained micrographs and B) relative adhesion of Saos-2 cells on PEG (w/o peptide nanofibers) and PEG-peptide (E_3-PA combination) substrates at 24 h in serum free culture conditions.

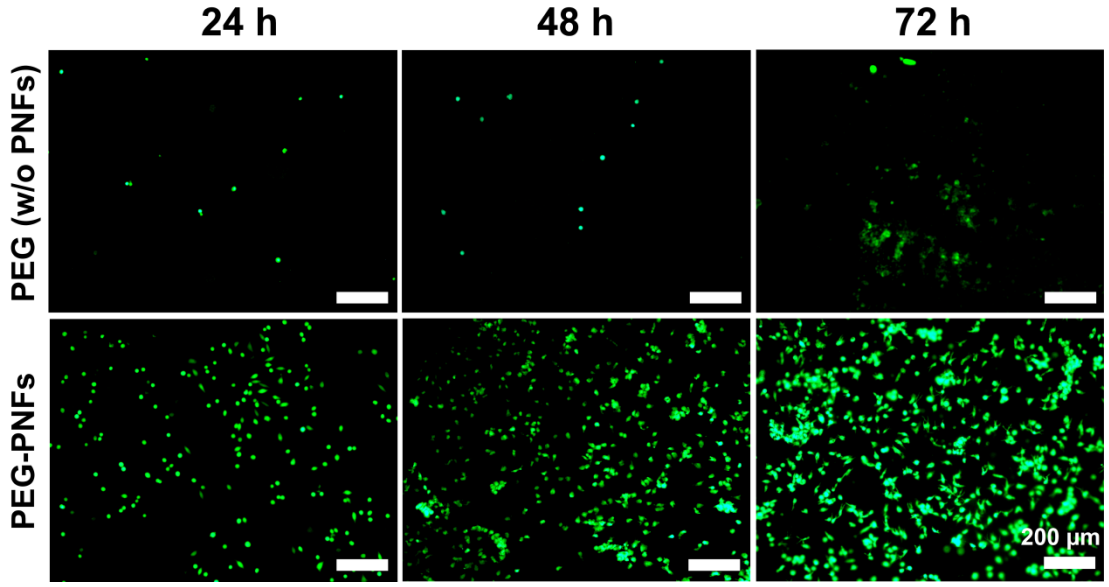

Figure 2.14. Representative Calcein-AM stained micrographs of Saos-2 cells on PEG (w/o peptide nanofibers) samples and PEG-peptide (E_3-PEG with 12% wt PEGDMA) composites showing the enhanced adhesion of cells with peptide incorporation.

2.3.5.3. Spreading and Cytoskeletal Organization Analysis

To further characterize the cell-material interactions, F-actin staining was performed for the evaluation of cell morphologies on the hydrogel surfaces. Cells on PEG (w/o peptide nanofibers) hydrogels retained a spherical morphology regardless of mechanical properties while the ones on PEG-peptide composites prefered to spread out on the surface (Figure 2.15). Quantitative analysis confirmed extensive spreading of cells on all of the PEG-peptide composites when compared to PEG (w/o peptide nanofibers) control (Figure 2.16A). Incorporation of peptide nanofibers within the crosslinked PEG system, suppressed the protein-repellent property of PEG and supported cell-material

interactions. Additionally, the superior effect of RGD epitope was clear. Spreading area of cells on RGD-PEG was significantly higher then other peptide combinations for all of the soft, medium and stiff hydrogels. An interesting finding was the synergistic effect between the mechanical properties and bioactive signals. In case of the integrin binding epitopes, projected spreading area of cells was increased in correlation with the increasing stiffness. On the stiff hydrogels presenting RGD and DGEA epitopes, extensive spreading (Figure 2.16A) and increase in the cell aspect ratios (Figure 2.16B) were observed when compared to their soft and medium states while no change was observed for non-integrin binding E_3-PEG hydrogel. Consequently, the cellular response to the material was affected not only by the mechanical properties, but also by the presence of bioactive signalling sequences. Associated with their ability to allow independent control of mechanical and biochemical properties, PEG-peptide composite hydrogels provided a versatile platform for the manipulation of cell interactions with the material.

2.3.5.4. Gene Expression Analysis

In the natural ECM environment, cells receive complex signals which interact with each other to create a combined effect on the orientation of cellular behaviour. Since both biochemical and biophysical properties of a material can affect cell fate, it is difficult to provide a scaffold that optimally stimulates differentiation and tissue regeneration with the utilization of current uni-functional strategies. Our hydrogel system can serve as a multifunctional platform to direct cell behaviour according to desired outcome. For this purpose, we

investigated the combined effect of complex niche cues on osteogenic commitment of Saos-2 cells. To analyze the osteoinductive effect of varied substrate stiffness and biochemical signals, gene expression profiles of runt-related transcription factor 2 (RUNX2) and collagen type I (COL1) were explored. Primer list used in the qRT-PCR setups is given at Table 2.3.

Table 2.3. Primer list used in the qRT-PCR setups.

	Forward Primer	**Reverse Primer**
RUNX2	5'-TCTGGCCTTCCACTCTCAGT-3'	5'-GACTGGCGGGGTGTAAGTAA-3'
COL1	5'-GAGAGCATGACCGATGGATT-3'	5'-CCTTCTTGAGGTTGCCAGTC-3'
GAPDH	5'- TCGACAGTCAGCCGCATCTTCT-3'	5'-GTGACCAGGCGCCCAATACGAC-3'

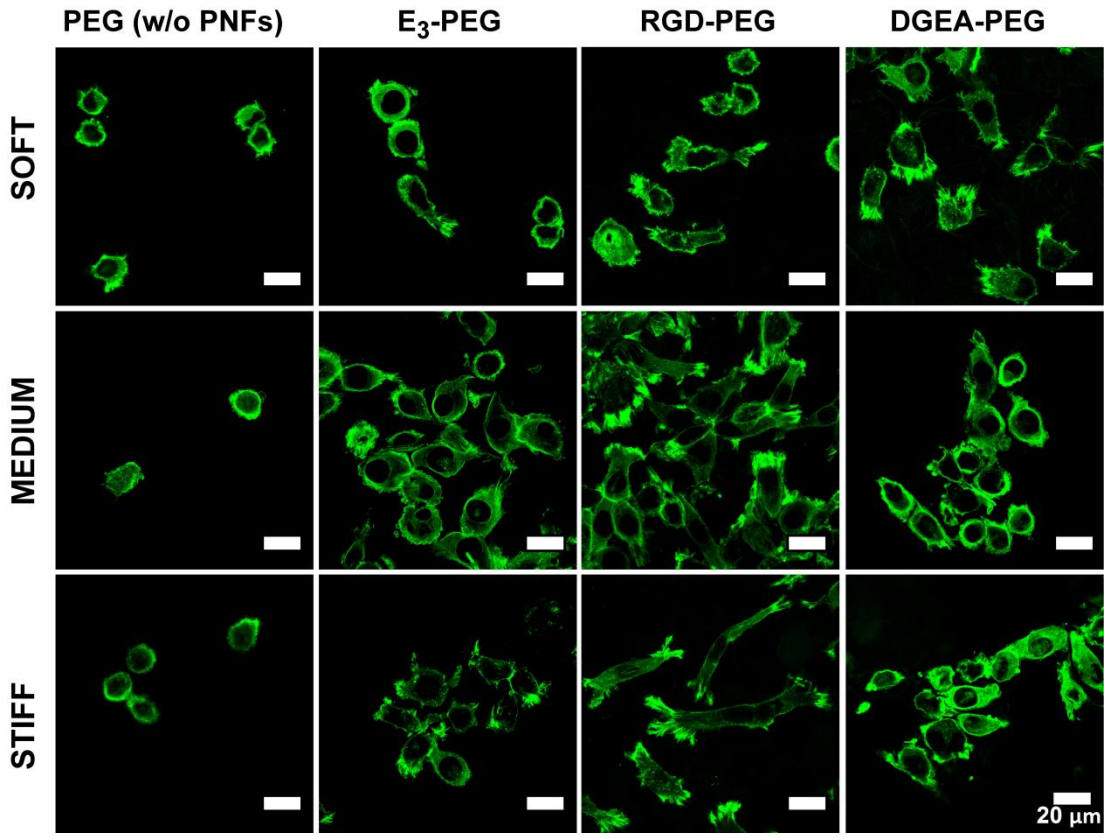

Figure 2.15. Representative Phalloidin stained micrographs of Saos-2 cells on PEG (w/o peptide nanofibers) and PEG-peptide substrates at 72 h.

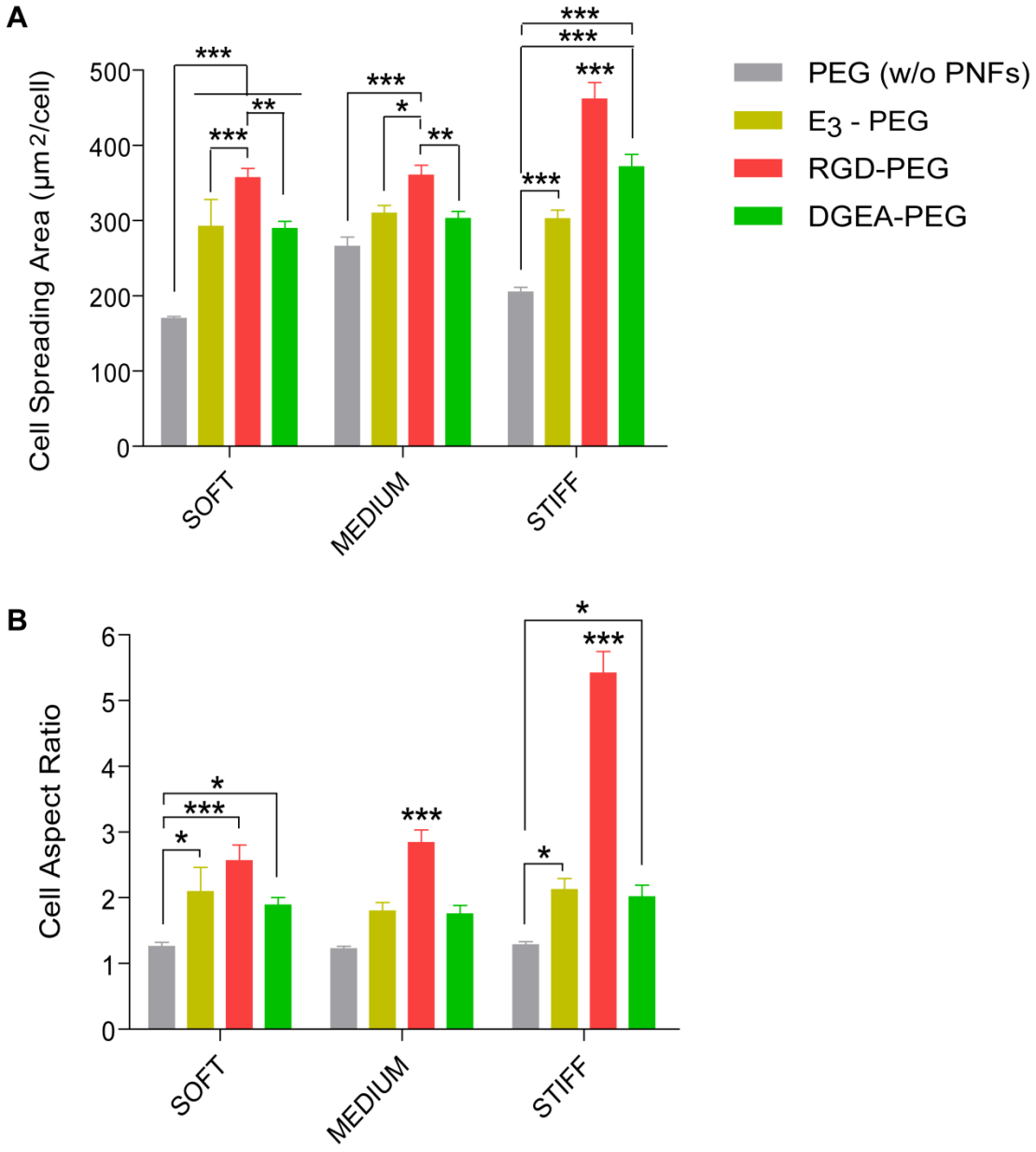

Figure 2.16. A) Projected spreading areas and B) aspect ratios of Saos-2 cells on PEG (w/o peptide nanofibers) and PEG-peptide substrates at 72 h.

2.3.5.4.1. ICC Staining

Gene expression profiles were qualitatively analyzed with ICC staining. ICC stained micrographs for RUNX2 and COL1, showed that each gene was expressed on all of the PEG (w/o peptide nanofibers) and PEG-peptide hydrogel combinations (Figure 2.17).

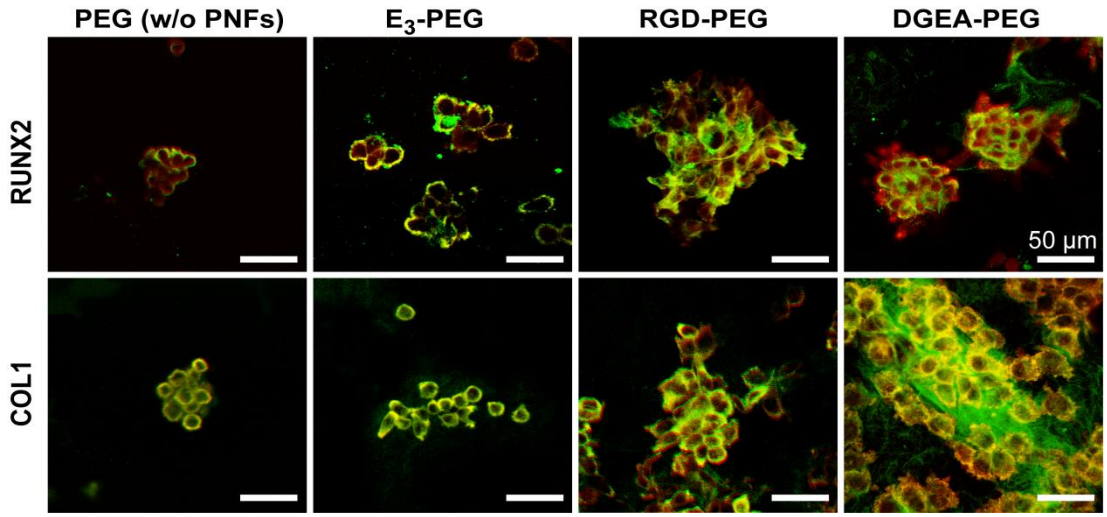

Figure 2.17. Representative ICC micrographs (40X magnification) of Saos-2 cells on crosslinked PEG (w/o peptide nanofibers) and PEG-peptide composite substrates at day 7. Green: Runx-2, Red: Phalloidin.

2.3.5.4.2. qRT-PCR Analysis

To quantitatively analyze the gene expression levels, qRT-PCR analysis was conducted. Independent from the biochemical signalling epitopes, stiffness of the PEG (w/o peptide nanofibers) alone affected the osteogenic lineage commitment of Saos-2 cells. For the early stage of osteogenic differentiation, RUNX2 and COL1 gene expressions were incrased along with the residual gel stiffness at day 3 (Figure 2.18A, Figure 2.18C). It is a known fact that cells adjust their

cytoskeletal organization according to the differences in substrate stiffness. The organization of cytoskeleton determines the shape of a cell and ultimately effects cellular behaviour.[139,190] As seen from Calcein stained micrographs of Saos-2 cells on day 3 of cultivation, cells preferred to come together and form clusters on PEG (w/o peptide nanofibers) hydrogels, since they can not generate any cell-material contact to attach the surface due to the protein-repellent property of PEG (Figure 2.12). The size of the consisted cell clusters was in a linear relationship with the increasing substrate stiffness. Cells on the soft gels formed smaller clusters, while the ones on the medium and stiff gels formed larger clusters. The validity of the fact that cell morphology can regulate differentiation was clearly demonstrated by previous studies. In one example, Chen and co-workers cultured stem cells on adhesive islands with different sizes. Cells on smaller islands differentiated into adipogenic lineage in contrast to the ones that went under osteogenic differentiation on larger islands.[191] Similarly, our results supported that the morphology and cellular organization can determine cell fate. Along with increasing substrate stiffness, formation of larger cell clusters on PEG (w/o peptide nanofibers) hydrogels enhanced the commitment of Saos-2 cells into osteogenic lineage and resulted in upregulated RUNX2 and COL1 gene expressions at the early stage of differentiation.

A similar result was obtained for non-integrin binding E_3-PEG substrate. Both on day 3 and day 7, highest RUNX2 gene expression was observed on E_3-PEG hydrogel groups and the expression level was increased along with increasing stiffness (Figure 2.18A, Figure 2.18B). Also, COL1 gene expression was at the

highest level on medium E_3-PEG substrates compared to integrin binding RGD-PEG and DGEA-PEG groups as well as non-bioactive PEG (w/o peptide nanofibers) control (Figure 2.18C, 2.18D). Even though EEE (E_3) is not an integrin binding peptide sequence, osteoinductive effect of E_3-PA with its ability to mimic acidic residues in non-collagenous matrix proteins, was previously assessed by our group.[192] A combinational approach of E_3-PA and DGEA-PA along with mussel-adhesive protein containing DOPA-PA resulted in enhanced osteogenic differentiation similarly to results. RUNX2 and COL1 gene expressions of human mesenchymal stem cells were elevated on E_3-PA/DOPA-PA hydrogel in comparison to DGEA-PA/DOPA-PA combination. In our case, presentation of E_3 peptide epitope within the PEG matrix resulted in the enhanced osteogenic differentiation of Saos-2 cells with the preference of increased stiffness.

Combination of integrin-binding epitopes with variable mechanical stiffness resulted in a non-typical differentiation behaviour compared to non-bioactive PEG (w/o peptide nanofibers) and non-integrin binding E_3-PEG. Instead of gradual increase of gene expression levels linear to increasing substrate stiffness, integrin binding RGD-PEG and DGEA-PEG combinations exhibited different patterns for osteogenic differentiation. Gene expression profile of RGD-PEG group was not affected by the mechanical properties and similar expression levels were obtained for all of the soft, medium and stiff hydrogel groups. Any upregulation of RUNX2 was not observed while COL1 gene expression was increased upto 6 fold on RGD-PEG combinations independent from substrate

stiffness on day 3 (Figure 2.18A & Figure 2.18C). Moreover, soft and stiff DGEA-PEG combinations presented higher expression of RUNX2 and COL1 (Figure 2.18) compared to medium DGEA-PEG. These results confirmed the presence of an interactive effect between integrin signalling and mechanical stimuli. Only few studies investigated the combined effects of biochemical and biophysical factors on cell behaviour. Nevertheless, it is known that in the presence of complex niche cues, cell morphology, substrate stiffness and biochemical signalling can supersede each other under certain conditions.[95,191] As in our case, a multifunctional scaffold system can alter different integrin related signalling pathways within the cells, therefore further investigation is needed to clarify the underlying mechanism of this behaviour. However, the preference soft and stiff combinations for DGEA-PEG combination might be explained by previously elucidated factors related to osteoblast differentiation. DGEA is a collagen type I derived signalling sequence that binds to $\alpha_2\beta_1$ integrin receptor. α_2-integrin is known as an early mechanotransducer of matrix elasticity in osteogenic cells and the increased expression of α_2-integrin of the cell membrane on stiffer matrices was already demonstrated.[193] Along with increased stiffness, upregulated α_2-integrin expression of cells can lead to a more pronounced effect of DGEA signalling on osteoblast differentiation. On the other hand, during bone development, cellular differentiation into bone forming osteoblasts occurs within a soft matrix in the range of 100-1000 Pa shear modulus.[194-195] Previous studies also introduced that *in vitro* osteogenic differentiation can be supported on soft hydrogel matrices which have a similar stiffness to intramembranous ossification of developing bone.[196-197]

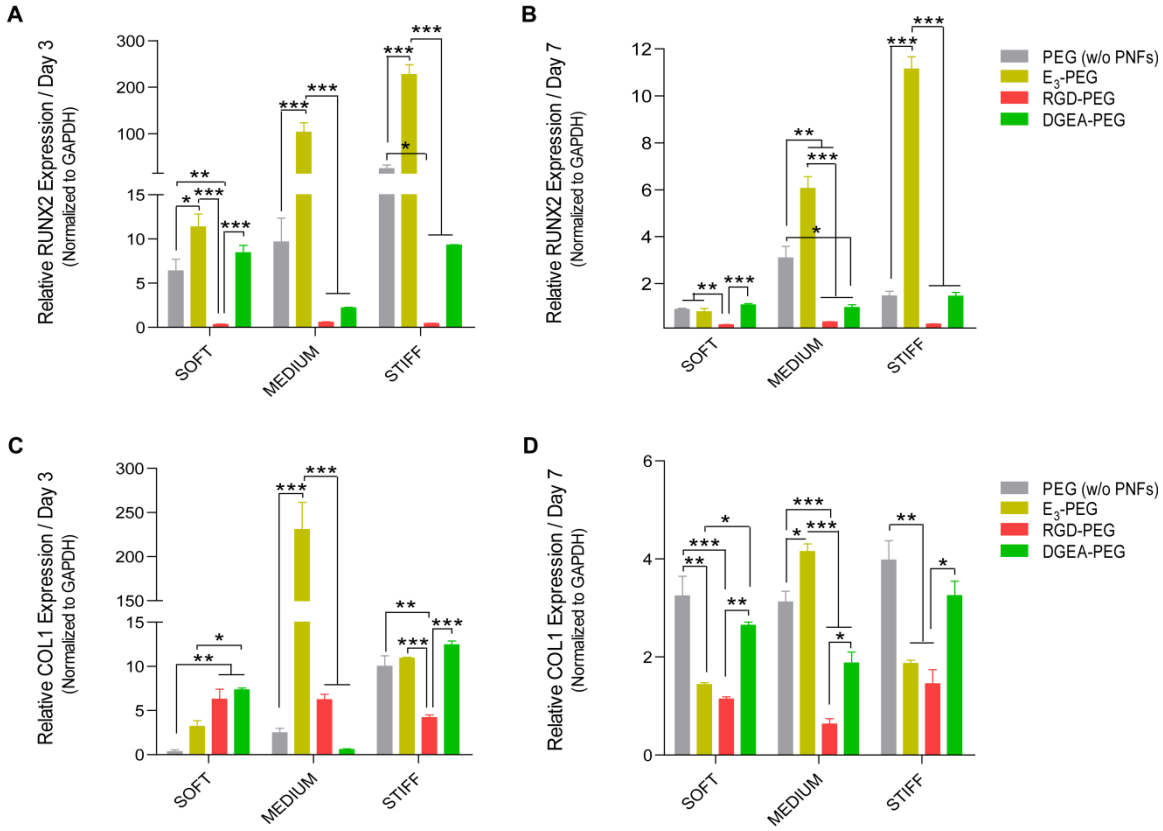

Figure 2.18. A,B) RUNX2 and C,D) COL1 gene expressions of Saos-2 cells on crosslinked PEG (w/o peptide nanofibers) and PEG-peptide composite substrates at day 3 and day 7.

Consequently, gene expression results obtained from our composite system confirmed that the optimal design of a material for the desired cellular outcome requires the consideration of multiple factors since cells can sense complex niche cues. These multifactorial signals can direct cell fate in an interactive manner.

2.3.6. Preperation of 3D Hydrogels

Current strategies to introduce porosity into 3D scaffolds such as electrospinning, freze-drying, gas foaming and salt leaching, are usually performed under non-physiological conditions.[171-172,198-199] Therefore, the biomedical applications of these systems only allow for cell seeding after the fabrication process, and as a result, non-uniform cell distribution can rise up as a problem. As a proof of concept, we also wanted to test the capability of our porous composite matrices as 3D platforms that allow for a cell-friendly fabrication process and *in situ* application of engineered scaffolds. To confirm the cell supportive effect of porosity within our 3D scaffold systems, PEG (w/o peptide nanofibers) versus RGD-PEG combinations were compared. For this purpose, similar simple preparation approach was applied to encapsulate Saos-2 cells into 3D matrices. Only difference was that all peptide and PEG-photoinitiator solutions were prepared with culture medium (DMEM) instead of water and cell suspension was mixed with PEG solution before the addition of PA solutions into the mixture. After the preperation of pre-gel solutions, mixtures were transferred into the caps of eppendorf tubes and exposed to UV light at 365 nm for 15 min.

2.3.6.1. Viability Analysis within the 3D Hydrogels

The resulting disc-shaped 3D gels containing encapsulated Saos-2 cells were cultured in a Synthecon RCCS-4H bioreactor with rotating vessels. After 7 days of cultivation, live/dead assay was performed to asses the viability of cells in 3D scaffolds. Cells within the porous RGD-PEG composite scaffolds were stained with Calcein-AM indicating the alive cells while the ones inside the non-porous

PEG (w/o peptide nanofibers) hydrogel stained with ethidium homodimer indicating the dead cells (Figure 2.19). Even though we did not observe any cytotoxic effect of PEG (w/o peptide nanofibers) hydrogel as a 2D scaffold, deficieny of porosity terminally affected the cell viability under 3D conditions. On the other hand, no detrimental effects on cell viability were observed within RGD-PEG scaffold. The increased porosity of our composite scaffolds supported the cell viability within the 3D matrix due to its ability to provide diffusion of neccessary nutrients and carbon dioxide. This result demonstrated the versatility of our novel multifunctional PEG-peptide composite system as a 3D platform for cell culture.

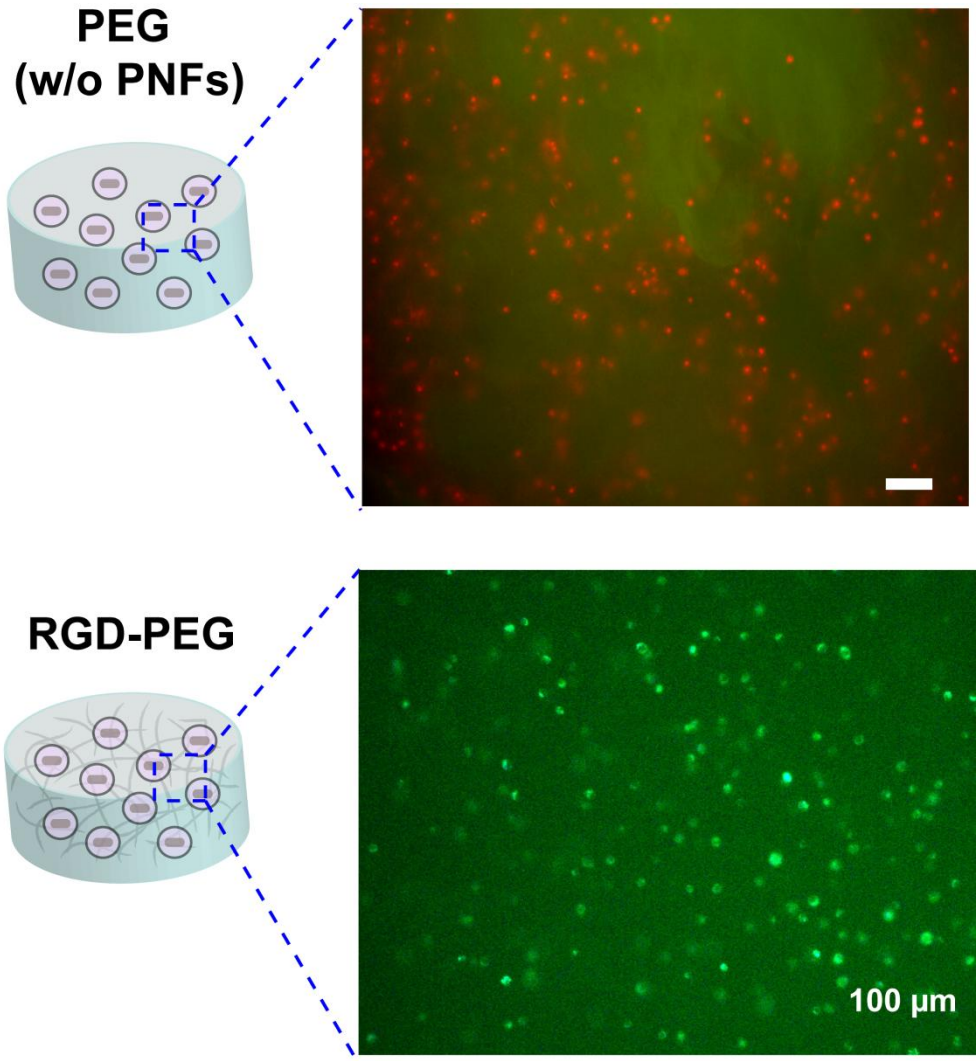

Figure 2.19. Representative live/dead micrographs of Saos-2 cells encapsulated within three-dimensional (top) PEG (w/o peptide nanofibers) and (bottom) RGD-PEG scaffolds at day 7. Green: Calcein-AM indicating the alive cells; Red: Ethidium homodimer indicating the dead cells.

2.4. CONCLUSION & FUTURE PERSPECTIVES

In summary, here we reported the design, synthesis and application of a PEG-peptide based composite platform to create multifunctional hydrogel systems which can be utilized as synthetic ECM analogues with multiple niche properties. Presented design enables independent control of mechanical and biochemical cues of the hydrogels without the modification of PEG backbone. Such a multifunctional hydrogel system can be modified through fine tuning of its properties to produce optimal scaffold compositions for the modulation of cellular processes according to the desired type of tissue engineering applications. Meanwhile, combining the self-assembled peptide nanofibers with the crosslinked PEG network resulted in formation of porous hydrogel systems without complex chemical modifications. Easy fabrication process under physiological conditions supported cell viability within 3D matrix more closely to real ECM environment that the cells feel, and can further allow the *in situ* applications of our system. Our strategy offers a facile fabrication method for mechanical and biochemical functionalization of hydrogels via incorporation of non-covalently self-assembled peptide nanofibers within the covalently crosslinked polymer network. Bioactive functionalization can be extended according to the complexity of target tissue. Ultimately, the resulting hydrogel system could provide a valuable tool that permits the investigation of how complex niche cues interplay to influence cellular behaviour and tissue formation within 3D conditions as well as on 2D material platforms. The simplicity of the system can further allow creation of precisely controlled and variable synthetic environments to be utilized in multiple disciplines including physics, biology and engineering.

Bibliography

1. Kleinman, H.K., Philp, D. & Hoffman, M.P. Role of the extracellular matrix in morphogenesis. *Curr Opin Biotechnol* **14**, 526-532 (2003).
2. Rosso, F., Giordano, A., Barbarisi, M. & Barbarisi, A. From cell-ECM interactions to tissue engineering. *J Cell Physiol* **199**, 174-180 (2004).
3. Cukierman, E., Pankov, R., Stevens, D.R. & Yamada, K.M. Taking cell-matrix adhesions to the third dimension. *Science* **294**, 1708-1712 (2001).
4. Berrier, A.L. & Yamada, K.M. Cell-matrix adhesion. *J Cell Physiol* **213**, 565-573 (2007).
5. Lund, A.W., Yener, B., Stegemann, J.P. & Plopper, G.E. The natural and engineered 3D microenvironment as a regulatory cue during stem cell fate determination. *Tissue Eng Part B Rev* **15**, 371-380 (2009).
6. Owen, S.C. & Shoichet, M.S. Design of three-dimensional biomimetic scaffolds. *J Biomed Mater Res A* **94**, 1321-1331 (2010).
7. Mecham, R.P. Overview of extracellular matrix. *Curr Protoc Cell Biol* **Chapter 10**, Unit 10 11 (2012).
8. Gieni, R.S. & Hendzel, M.J. Mechanotransduction from the ECM to the genome: are the pieces now in place? *J Cell Biochem* **104**, 1964-1987 (2008).
9. Badylak, S.F. The extracellular matrix as a biologic scaffold material. *Biomaterials* **28**, 3587-3593 (2007).
10. von der Mark, K., Sorokin, L. (ed.) *Adhesive glycoproteins*, 293-328 (Wiley-Liss, New York, 2002).
11. Rossert, J., de Crombrugghe, B., John, P.B., Lawrence, G.R., Gideon, A.R. *Type I Collagen: Structure, Synthesis, and Regulation, Principles of Bone Biology*, (Academic Press, San Diego, 2002).
12. Robey, P.G., John, P.B., Lawrence, G.R., Gideon, A.R. *Bone Matrix Proteoglycans and Glycoproteins, Principle of Bone Biology*, (Academic Press, San Diego, 2002).
13. Zhang, H., *et al.* Profiling genes expressed in human fetal cartilage using 13,155 expressed sequence tags. *Osteoarthritis Cartilage* **11**, 309-319 (2003).
14. Muiznieks, L.D. & Keeley, F.W. Molecular assembly and mechanical properties of the extracellular matrix: A fibrous protein perspective. *Biochim Biophys Acta* **1832**, 866-875 (2013).
15. Shadwick, R.E. Elastic energy storage in tendons: mechanical differences related to function and age. *J Appl Physiol (1985)* **68**, 1033-1040 (1990).
16. Shoulders, M.D. & Raines, R.T. Collagen structure and stability. *Annu Rev Biochem* **78**, 929-958 (2009).
17. Gordon, M.K. & Hahn, R.A. Collagens. *Cell Tissue Res* **339**, 247-257 (2010).

18. Wess, T.J. Collagen fibril form and function. *Adv Protein Chem* **70**, 341-374 (2005).
19. Brinckmann, J., Notbohm, H., Müller, P. *Collagen-primer in structure, processing and assembly*, (Springer, Berlin, 2005).
20. Fratzl, P. *Collagen: structure and mechanics*, (Springer, Berlin, 2008).
21. Kielty, C.M., Grant, M. (ed.) *The collagen family: structure, assembly, and organization in the extracellular matrix*, 159-221 (New York, Wiley-Liss, 2002).
22. Khoshnoodi, J., Pedchenko, V. & Hudson, B.G. Mammalian collagen IV. *Microsc Res Tech* **71**, 357-370 (2008).
23. Stephan, S., Sherratt, M.J., Hodson, N., Shuttleworth, C.A. & Kielty, C.M. Expression and supramolecular assembly of recombinant alpha1(viii) and alpha2(viii) collagen homotrimers. *J Biol Chem* **279**, 21469-21477 (2004).
24. Kwan, A.P., Cummings, C.E., Chapman, J.A. & Grant, M.E. Macromolecular organization of chicken type X collagen in vitro. *J Cell Biol* **114**, 597-604 (1991).
25. Kadler, K.E., Baldock, C., Bella, J. & Boot-Handford, R.P. Collagens at a glance. *J Cell Sci* **120**, 1955-1958 (2007).
26. Hynes, R. *Fibronectins*, Springer (1990).
27. Potts, J.R. & Campbell, I.D. Fibronectin structure and assembly. *Curr Opin Cell Biol* **6**, 648-655 (1994).
28. Xu, J., Mocher, D. (ed.) *Fibronectin and Other Adhesive Glycoproteins*, Springer-Verlag, Berlin Heidelberg, 41-70 (2011).
29. Preissner, K.T. Structure and biological role of vitronectin. *Annu Rev Cell Biol* **7**, 275-310 (1991).
30. Brooks, P.C., Clark, R.A. & Cheresh, D.A. Requirement of vascular integrin alpha v beta 3 for angiogenesis. *Science* **264**, 569-571 (1994).
31. Nishimura, S.L., Sheppard, D. & Pytela, R. Integrin alpha v beta 8. Interaction with vitronectin and functional divergence of the beta 8 cytoplasmic domain. *J Biol Chem* **269**, 28708-28715 (1994).
32. Schnapp, L.M., *et al.* The human integrin alpha 8 beta 1 functions as a receptor for tenascin, fibronectin, and vitronectin. *J Biol Chem* **270**, 23196-23202 (1995).
33. Smith, J.W. & Cheresh, D.A. Integrin (alpha v beta 3)-ligand interaction. Identification of a heterodimeric RGD binding site on the vitronectin receptor. *J Biol Chem* **265**, 2168-2172 (1990).
34. Thiagarajan, P. & Kelly, K. Interaction of thrombin-stimulated platelets with vitronectin (S-protein of complement) substrate: inhibition by a monoclonal antibody to glycoprotein IIb-IIIa complex. *Thromb Haemost* **60**, 514-517 (1988).

35. Felding-Habermann, B. & Cheresh, D.A. Vitronectin and its receptors. *Curr Opin Cell Biol* **5**, 864-868 (1993).
36. Meredith, J.E., Jr., *et al.* The regulation of growth and intracellular signaling by integrins. *Endocr Rev* **17**, 207-220 (1996).
37. Savill, J., Dransfield, I., Hogg, N. & Haslett, C. Vitronectin receptor-mediated phagocytosis of cells undergoing apoptosis. *Nature* **343**, 170-173 (1990).
38. Schwartz, M.A. & Assoian, R.K. Integrins and cell proliferation: regulation of cyclin-dependent kinases via cytoplasmic signaling pathways. *J Cell Sci* **114**, 2553-2560 (2001).
39. Nishiuchi, R., *et al.* Ligand-binding specificities of laminin-binding integrins: a comprehensive survey of laminin-integrin interactions using recombinant alpha3beta1, alpha6beta1, alpha7beta1 and alpha6beta4 integrins. *Matrix Biol* **25**, 189-197 (2006).
40. Patarroyo, M., Tryggvason, K. & Virtanen, I. Laminin isoforms in tumor invasion, angiogenesis and metastasis. *Semin Cancer Biol* **12**, 197-207 (2002).
41. Watt, F.M. Role of integrins in regulating epidermal adhesion, growth and differentiation. *EMBO J* **21**, 3919-3926 (2002).
42. Givant-Horwitz, V., Davidson, B. & Reich, R. Laminin-induced signaling in tumor cells. *Cancer Lett* **223**, 1-10 (2005).
43. Gonzales, M., *et al.* A cell signal pathway involving laminin-5, alpha3beta1 integrin, and mitogen-activated protein kinase can regulate epithelial cell proliferation. *Mol Biol Cell* **10**, 259-270 (1999).
44. Hintermann, E. & Quaranta, V. Epithelial cell motility on laminin-5: regulation by matrix assembly, proteolysis, integrins and erbB receptors. *Matrix Biol* **23**, 75-85 (2004).
45. Roberts, D.D., Lau, L.F. (ed.) *Matricellular proteins*, 369-413 (Springer, Berlin, 2011).
46. Heinegard, D. & Sommarin, Y. Proteoglycans: an overview. *Methods Enzymol* **144**, 305-319 (1987).
47. Iozzo, R.V. Matrix proteoglycans: from molecular design to cellular function. *Annu Rev Biochem* **67**, 609-652 (1998).
48. Hardingham, T. & Bayliss, M. Proteoglycans of articular cartilage: changes in aging and in joint disease. *Semin Arthritis Rheum* **20**, 12-33 (1990).
49. Hedbom, E. & Heinegard, D. Binding of fibromodulin and decorin to separate sites on fibrillar collagens. *J Biol Chem* **268**, 27307-27312 (1993).
50. Hausser, H., Groning, A., Hasilik, A., Schonherr, E. & Kresse, H. Selective inactivity of TGF-beta/decorin complexes. *FEBS Lett* **353**, 243-245 (1994).

51. Schaefer, L. & Iozzo, R.V. Biological functions of the small leucine-rich proteoglycans: from genetics to signal transduction. *J Biol Chem* **283**, 21305-21309 (2008).
52. Vogel, W.F., Abdulhussein, R. & Ford, C.E. Sensing extracellular matrix: an update on discoidin domain receptor function. *Cell Signal* **18**, 1108-1116 (2006).
53. Hynes, R.O. Integrins: bidirectional, allosteric signaling machines. *Cell* **110**, 673-687 (2002).
54. Schwartz, M.A. Integrin signaling revisited. *Trends Cell Biol* **11**, 466-470 (2001).
55. Humphries, J.D., Byron, A. & Humphries, M.J. Integrin ligands at a glance. *J Cell Sci* **119**, 3901-3903 (2006).
56. Arnaout, M.A. Integrin structure: new twists and turns in dynamic cell adhesion. *Immunol Rev* **186**, 125-140 (2002).
57. Humphries, M.J., *et al.* Integrin structure: heady advances in ligand binding, but activation still makes the knees wobble. *Trends Biochem Sci* **28**, 313-320 (2003).
58. Takagi, J., Petre, B.M., Walz, T. & Springer, T.A. Global conformational rearrangements in integrin extracellular domains in outside-in and inside-out signaling. *Cell* **110**, 599-511 (2002).
59. Grashoff, C., Aszodi, A., Sakai, T., Hunziker, E.B. & Fassler, R. Integrin-linked kinase regulates chondrocyte shape and proliferation. *EMBO Rep* **4**, 432-438 (2003).
60. Guo, W. & Giancotti, F.G. Integrin signalling during tumour progression. *Nat Rev Mol Cell Biol* **5**, 816-826 (2004).
61. Legate, K.R., Wickstrom, S.A. & Fassler, R. Genetic and cell biological analysis of integrin outside-in signaling. *Genes Dev* **23**, 397-418 (2009).
62. Arnaout, M.A., Goodman, S.L. & Xiong, J.P. Structure and mechanics of integrin-based cell adhesion. *Curr Opin Cell Biol* **19**, 495-507 (2007).
63. Petit, V. & Thiery, J.P. Focal adhesions: structure and dynamics. *Biol Cell* **92**, 477-494 (2000).
64. Giancotti, F.G. & Ruoslahti, E. Integrin signaling. *Science* **285**, 1028-1032 (1999).
65. Giancotti, F.G. A structural view of integrin activation and signaling. *Dev Cell* **4**, 149-151 (2003).
66. Hynes, R.O. Integrins: versatility, modulation, and signaling in cell adhesion. *Cell* **69**, 11-25 (1992).
67. Pytela, R., Pierschbacher, M.D., Argraves, S., Suzuki, S. & Ruoslahti, E. Arginine-glycine-aspartic acid adhesion receptors. *Methods Enzymol* **144**, 475-489 (1987).

68. Arnaout, M.A., Mahalingam, B. & Xiong, J.P. Integrin structure, allostery, and bidirectional signaling. *Annu Rev Cell Dev Biol* **21**, 381-410 (2005).
69. Pytela, R., Pierschbacher, M.D. & Ruoslahti, E. Identification and isolation of a 140 kd cell surface glycoprotein with properties expected of a fibronectin receptor. *Cell* **40**, 191-198 (1985).
70. Eble, J.A. The molecular basis of integrin-extracellular matrix interactions. *Osteoarthritis Cartilage* **9 Suppl A**, S131-140 (2001).
71. Emsley, J., Knight, C.G., Farndale, R.W. & Barnes, M.J. Structure of the integrin alpha2beta1-binding collagen peptide. *J Mol Biol* **335**, 1019-1028 (2004).
72. Sasaki, T. & Timpl, R. Domain IVa of laminin alpha5 chain is cell-adhesive and binds beta1 and alphaVbeta3 integrins through Arg-Gly-Asp. *FEBS Lett* **509**, 181-185 (2001).
73. Tashiro, K., *et al.* The RGD containing site of the mouse laminin A chain is active for cell attachment, spreading, migration and neurite outgrowth. *J Cell Physiol* **146**, 451-459 (1991).
74. Graf, J., *et al.* A pentapeptide from the laminin B1 chain mediates cell adhesion and binds the 67,000 laminin receptor. *Biochemistry* **26**, 6896-6900 (1987).
75. Grant, D.S., *et al.* Two different laminin domains mediate the differentiation of human endothelial cells into capillary-like structures in vitro. *Cell* **58**, 933-943 (1989).
76. Tashiro, K., *et al.* A synthetic peptide containing the IKVAV sequence from the A chain of laminin mediates cell attachment, migration, and neurite outgrowth. *J Biol Chem* **264**, 16174-16182 (1989).
77. Humphries, M.J., Akiyama, S.K., Komoriya, A., Olden, K. & Yamada, K.M. Identification of an alternatively spliced site in human plasma fibronectin that mediates cell type-specific adhesion. *J Cell Biol* **103**, 2637-2647 (1986).
78. Komoriya, A., *et al.* The minimal essential sequence for a major cell type-specific adhesion site (CS1) within the alternatively spliced type III connecting segment domain of fibronectin is leucine-aspartic acid-valine. *J Biol Chem* **266**, 15075-15079 (1991).
79. Aota, S., Nomizu, M. & Yamada, K.M. The short amino acid sequence Pro-His-Ser-Arg-Asn in human fibronectin enhances cell-adhesive function. *J Biol Chem* **269**, 24756-24761 (1994).
80. McCann, T.J., Mason, W.T., Meikle, M.C. & McDonald, F. A collagen peptide motif activates tyrosine kinase-dependent calcium signalling pathways in human osteoblast-like cells. *Matrix Biol* **16**, 273-283 (1997).
81. Kleinman, H.K., *et al.* Identification of a second active site in laminin for promotion of cell adhesion and migration and inhibition of in vivo melanoma lung colonization. *Arch Biochem Biophys* **272**, 39-45 (1989).

82. Hynes, R.O. The extracellular matrix: not just pretty fibrils. *Science* **326**, 1216-1219 (2009).
83. Urry, D.W., *et al.* Elastin: a representative ideal protein elastomer. *Philos Trans R Soc Lond B Biol Sci* **357**, 169-184 (2002).
84. Fung, Y.C. *Biomechanics: Mechanical Properties of Liniving Tissues*, (Springer-Verlag, New York, 1981).
85. Elkin, B.S., Azeloglu, E.U., Costa, K.D. & Morrison, B., 3rd. Mechanical heterogeneity of the rat hippocampus measured by atomic force microscope indentation. *J Neurotrauma* **24**, 812-822 (2007).
86. Engler, A.J., *et al.* Myotubes differentiate optimally on substrates with tissue-like stiffness: pathological implications for soft or stiff microenvironments. *J Cell Biol* **166**, 877-887 (2004).
87. Lu, Y.B., *et al.* Viscoelastic properties of individual glial cells and neurons in the CNS. *Proc Natl Acad Sci U S A* **103**, 17759-17764 (2006).
88. Discher, D.E., Janmey, P. & Wang, Y.L. Tissue cells feel and respond to the stiffness of their substrate. *Science* **310**, 1139-1143 (2005).
89. Shao, Y. & Fu, J. Integrated micro/nanoengineered functional biomaterials for cell mechanics and mechanobiology: a materials perspective. *Adv Mater* **26**, 1494-1533 (2014).
90. Wang, N., Butler, J.P. & Ingber, D.E. Mechanotransduction across the cell surface and through the cytoskeleton. *Science* **260**, 1124-1127 (1993).
91. Missirlis, D. & Spatz, J.P. Combined Effects of PEG Hydrogel Elasticity and Cell-Adhesive Coating on Fibroblast Adhesion and Persistent Migration. *Biomacromolecules* **15**, 195-205 (2014).
92. Solon, J., Levental, I., Sengupta, K., Georges, P.C. & Janmey, P.A. Fibroblast adaptation and stiffness matching to soft elastic substrates. *Biophys J* **93**, 4453-4461 (2007).
93. Saez, A., Ghibaudo, M., Buguin, A., Silberzan, P. & Ladoux, B. Rigidity-driven growth and migration of epithelial cells on microstructured anisotropic substrates. *Proc Natl Acad Sci U S A* **104**, 8281-8286 (2007).
94. Hadjipanayi, E., Mudera, V. & Brown, R.A. Close dependence of fibroblast proliferation on collagen scaffold matrix stiffness. *J Tissue Eng Regen Med* **3**, 77-84 (2009).
95. Engler, A.J., Sen, S., Sweeney, H.L. & Discher, D.E. Matrix elasticity directs stem cell lineage specification. *Cell* **126**, 677-689 (2006).
96. Singh, A., Zhan, J.A., Ye, Z.Y. & Elisseeff, J.H. Modular Multifunctional Poly(ethylene glycol) Hydrogels for Stem Cell Differentiation. *Adv Funct Mater* **23**, 575-582 (2013).
97. Geiger B Fau - Bershadsky, A., Bershadsky A Fau - Pankov, R., Pankov R Fau - Yamada, K.M. & Yamada, K.M. Transmembrane crosstalk between the extracellular matrix--cytoskeleton crosstalk.

98. Yamada, K.M. & Miyamoto, S. Integrin transmembrane signaling and cytoskeletal control. *Current Opinion in Cell Biology* **7**, 681-689 (1995).
99. LaFlamme, S.E., Akiyama, S.K. & Yamada, K.M. Regulation of fibronectin receptor distribution. *J Cell Biol* **117**, 437-447 (1992).
100. Akiyama Sk Fau - Yamada, S.S., Yamada Ss Fau - Yamada, K.M., Yamada Km Fau - LaFlamme, S.E. & LaFlamme, S.E. Transmembrane signal transduction by integrin cytoplasmic domains expressed in single-subunit chimeras.
101. Lukashev Me Fau - Sheppard, D., Sheppard D Fau - Pytela, R. & Pytela, R. Disruption of integrin function and induction of tyrosine phosphorylation by the autonomously expressed beta 1 integrin cytoplasmic domain.
102. Ylänne, J., *et al.* Distinct functions of integrin alpha and beta subunit cytoplasmic domains in cell spreading and formation of focal adhesions. *The Journal of Cell Biology* **122**, 223-233 (1993).
103. Ingber, D.E. Tensegrity I. Cell structure and hierarchical systems biology. *J Cell Sci* **116**, 1157-1173 (2003).
104. Ingber, D.E. Tensegrity II. How structural networks influence cellular information processing networks. *J Cell Sci* **116**, 1397-1408 (2003).
105. Miyamoto S Fau - Teramoto, H., *et al.* Integrin function: molecular hierarchies of cytoskeletal and signaling molecules.
106. Maniotis, A.J., Chen, C.S. & Ingber, D.E. Demonstration of mechanical connections between integrins, cytoskeletal filaments, and nucleoplasm that stabilize nuclear structure. *Proceedings of the National Academy of Sciences* **94**, 849-854 (1997).
107. Itano, N., Okamoto, S., Zhang, D., Lipton, S.A. & Ruoslahti, E. Cell spreading controls endoplasmic and nuclear calcium: a physical gene regulation pathway from the cell surface to the nucleus. *Proceedings of the National Academy of Sciences of the United States of America* **100**, 5181-5186 (2003).
108. Lenhard, R.E., Osteen, R. T., Gansler, T.S. *American Cancer S. Clinical Oncology*, (American Cancer Society, Atlanta, 2001).
109. Venkatesan, J., Bhatnagar, I., Manivasagan, P., Kang, K.H. & Kim, S.K. Alginate composites for bone tissue engineering: A review. *Int J Biol Macromol* (2014).
110. Lieberman, J.R., Friedlander, G. E. *Bone Regeneration and Repair: Biology and Clinical Applications*, (Humana Press, Totowa, NJ, 2005).
111. Nguyen, K.T. & West, J.L. Photopolymerizable hydrogels for tissue engineering applications. *Biomaterials* **23**, 4307-4314 (2002).
112. Lutolf, M.P. & Hubbell, J.A. Synthetic biomaterials as instructive extracellular microenvironments for morphogenesis in tissue engineering. *Nat Biotechnol* **23**, 47-55 (2005).

113. Butcher, J.T. & Nerem, R.M. Porcine aortic valve interstitial cells in three-dimensional culture: comparison of phenotype with aortic smooth muscle cells. *J Heart Valve Dis* **13**, 478-485; discussion 485-476 (2004).
114. Burdick, J.A. & Prestwich, G.D. Hyaluronic acid hydrogels for biomedical applications. *Adv Mater* **23**, H41-56 (2011).
115. Ahmed, T.A., Dare, E.V. & Hincke, M. Fibrin: a versatile scaffold for tissue engineering applications. *Tissue Eng Part B Rev* **14**, 199-215 (2008).
116. Cadee, J.A., *et al.* In vivo biocompatibility of dextran-based hydrogels. *J Biomed Mater Res* **50**, 397-404 (2000).
117. Hughes, C.S., Postovit, L.M. & Lajoie, G.A. Matrigel: a complex protein mixture required for optimal growth of cell culture. *Proteomics* **10**, 1886-1890 (2010).
118. Cushing, M.C. & Anseth, K.S. Materials science. Hydrogel cell cultures. *Science* **316**, 1133-1134 (2007).
119. Sawhney, A.S., Pathak, C.P. & Hubbell, J.A. Bioerodible Hydrogels Based on Photopolymerized Poly(Ethylene Glycol)-Co-Poly(Alpha-Hydroxy Acid) Diacrylate Macromers. *Macromolecules* **26**, 581-587 (1993).
120. Martens, P. & Anseth, K.S. Characterization of hydrogels formed from acrylate modified poly(vinyl alcohol) macromers. *Polymer* **41**, 7715-7722 (2000).
121. Chirila, T.V., *et al.* Poly(2-hydroxyethyl methacrylate) sponges as implant materials: in vivo and in vitro evaluation of cellular invasion. *Biomaterials* **14**, 26-38 (1993).
122. Bryant, S.J. & Anseth, K.S. Hydrogel properties influence ECM production by chondrocytes photoencapsulated in poly(ethylene glycol) hydrogels. *J Biomed Mater Res* **59**, 63-72 (2002).
123. Zhu, J. Bioactive modification of poly(ethylene glycol) hydrogels for tissue engineering. *Biomaterials* **31**, 4639-4656 (2010).
124. Custodio, C.A., Reis, R.L. & Mano, J.F. Engineering biomolecular microenvironments for cell instructive biomaterials. *Adv Healthc Mater* **3**, 797-810 (2014).
125. Shin, H., Jo, S. & Mikos, A.G. Biomimetic materials for tissue engineering. *Biomaterials* **24**, 4353-4364 (2003).
126. Hynd, M.R., Frampton, J.P., Dowell-Mesfin, N., Turner, J.N. & Shain, W. Directed cell growth on protein-functionalized hydrogel surfaces. *J Neurosci Methods* **162**, 255-263 (2007).
127. Halstenberg, S., Panitch, A., Rizzi, S., Hall, H. & Hubbell, J.A. Biologically engineered protein-graft-poly(ethylene glycol) hydrogels: a cell adhesive and plasmin-degradable biosynthetic material for tissue repair. *Biomacromolecules* **3**, 710-723 (2002).

128. Massia, S.P. & Hubbell, J.A. Tissue engineering in the vascular graft. *Cytotechnology* **10**, 189-204 (1992).
129. Garcia, A.J. Get a grip: integrins in cell-biomaterial interactions. *Biomaterials* **26**, 7525-7529 (2005).
130. Hersel, U., Dahmen, C. & Kessler, H. RGD modified polymers: biomaterials for stimulated cell adhesion and beyond. *Biomaterials* **24**, 4385-4415 (2003).
131. Hern, D.L. & Hubbell, J.A. Incorporation of adhesion peptides into nonadhesive hydrogels useful for tissue resurfacing. *J Biomed Mater Res* **39**, 266-276 (1998).
132. Roberts, M.J., Bentley, M.D. & Harris, J.M. Chemistry for peptide and protein PEGylation. *Adv Drug Deliv Rev* **54**, 459-476 (2002).
133. Gobin, A.S. & West, J.L. Cell migration through defined, synthetic ECM analogs. *FASEB J* **16**, 751-753 (2002).
134. Burdick, J.A. & Anseth, K.S. Photoencapsulation of osteoblasts in injectable RGD-modified PEG hydrogels for bone tissue engineering. *Biomaterials* **23**, 4315-4323 (2002).
135. Salinas, C.N. & Anseth, K.S. Mixed mode thiol-acrylate photopolymerizations for the synthesis of PEG-peptide hydrogels. *Macromolecules* **41**, 6019-6026 (2008).
136. Liu, S.Q., *et al.* Injectable Biodegradable Poly(ethylene glycol)/RGD Peptide Hybrid Hydrogels for in vitro Chondrogenesis of Human Mesenchymal Stem Cells. *Macromol Rapid Comm* **31**, 1148-1154 (2010).
137. Mann, B.K., Tsai, A.T., Scott-Burden, T. & West, J.L. Modification of surfaces with cell adhesion peptides alters extracellular matrix deposition. *Biomaterials* **20**, 2281-2286 (1999).
138. Chen, C.S. Mechanotransduction - a field pulling together? *J Cell Sci* **121**, 3285-3292 (2008).
139. Yeung, T., *et al.* Effects of substrate stiffness on cell morphology, cytoskeletal structure, and adhesion. *Cell Motil Cytoskeleton* **60**, 24-34 (2005).
140. Engler, A.J., Sen, S., Sweeney, H.L. & Discher, D.E. Matrix elasticity directs stem cell lineage specification. *Cell* **126**, 677-689 (2006).
141. Santos, E., Hernandez, R.M., Pedraz, J.L. & Orive, G. Novel advances in the design of three-dimensional bio-scaffolds to control cell fate: translation from 2D to 3D. *Trends Biotechnol* **30**, 331-341 (2012).
142. Bryant, S.J., Bender, R.J., Durand, K.L. & Anseth, K.S. Encapsulating chondrocytes in degrading PEG hydrogels with high modulus: engineering gel structural changes to facilitate cartilaginous tissue production. *Biotechnol Bioeng* **86**, 747-755 (2004).
143. Saha, K., *et al.* Substrate modulus directs neural stem cell behavior. *Biophys J* **95**, 4426-4438 (2008).

144. Gilbert, P.M., *et al.* Substrate elasticity regulates skeletal muscle stem cell self-renewal in culture. *Science* **329**, 1078-1081 (2010).
145. Breuls, R.G., Jiya, T.U. & Smit, T.H. Scaffold stiffness influences cell behavior: opportunities for skeletal tissue engineering. *Open Orthop J* **2**, 103-109 (2008).
146. Lutolf, M.P. Integration column: artificial ECM: expanding the cell biology toolbox in 3D. *Integr Biol (Camb)* **1**, 235-241 (2009).
147. Stachowiak, A.N., Bershteyn, A., Tzatzalos, E. & Irvine, D.J. Bioactive hydrogels with an ordered cellular structure combine interconnected macroporosity and robust mechanical properties. *Advanced Materials* **17**, 399-+ (2005).
148. Keskar, V., Marion, N.W., Mao, J.J. & Gemeinhart, R.A. In Vitro Evaluation of Macroporous Hydrogels to Facilitate Stem Cell Infiltration, Growth, and Mineralization. *Tissue Eng Pt A* **15**, 1695-1707 (2009).
149. Lee, W., Cho, N.J., Xiong, A., Glenn, J.S. & Frank, C.W. Hydrophobic nanoparticles improve permeability of cell-encapsulating poly(ethylene glycol) hydrogels while maintaining patternability. *Proc Natl Acad Sci U S A* **107**, 20709-20714 (2010).
150. Dvir, T., Timko, B.P., Kohane, D.S. & Langer, R. Nanotechnological strategies for engineering complex tissues. *Nat Nanotechnol* **6**, 13-22 (2011).
151. Hartgerink, J.D., Beniash, E. & Stupp, S.I. Self-assembly and mineralization of peptide-amphiphile nanofibers. *Science* **294**, 1684-1688 (2001).
152. Cui, H., Webber, M.J. & Stupp, S.I. Self-assembly of peptide amphiphiles: from molecules to nanostructures to biomaterials. *Biopolymers* **94**, 1-18 (2010).
153. Zhang, S. Fabrication of novel biomaterials through molecular self-assembly. *Nat Biotechnol* **21**, 1171-1178 (2003).
154. Kloxin, A.M., Kloxin, C.J., Bowman, C.N. & Anseth, K.S. Mechanical properties of cellularly responsive hydrogels and their experimental determination. *Adv Mater* **22**, 3484-3494 (2010).
155. Langer, R. & Peppas, N.A. Advances in biomaterials, drug delivery, and bionanotechnology. *Aiche J* **49**, 2990-3006 (2003).
156. Thiele, J., Ma, Y., Bruekers, S.M., Ma, S. & Huck, W.T. 25th anniversary article: Designer hydrogels for cell cultures: a materials selection guide. *Adv Mater* **26**, 125-147 (2014).
157. Drury, J.L. & Mooney, D.J. Hydrogels for tissue engineering: scaffold design variables and applications. *Biomaterials* **24**, 4337-4351 (2003).
158. Lee, K.Y. & Mooney, D.J. Hydrogels for tissue engineering. *Chem Rev* **101**, 1869-1879 (2001).
159. Hoffman, A.S. Hydrogels for biomedical applications. *Adv Drug Deliv Rev* **54**, 3-12 (2002).

160. Kleinman, H.K., Philp, D. & Hoffman, M.P. Role of the extracellular matrix in morphogenesis. *Curr Opin Biotech* **14**, 526-532 (2003).
161. Wheeldon, I., Farhadi, A., Bick, A.G., Jabbari, E. & Khademhosseini, A. Nanoscale tissue engineering: spatial control over cell-materials interactions. *Nanotechnology* **22**(2011).
162. Giancotti, F.G. & Ruoslahti, E. Transduction - Integrin signaling. *Science* **285**, 1028-1032 (1999).
163. Cukierman, E., Pankov, R., Stevens, D.R. & Yamada, K.M. Taking cell-matrix adhesions to the third dimension. *Science* **294**, 1708-1712 (2001).
164. Palecek, S.P., Loftus, J.C., Ginsberg, M.H., Lauffenburger, D.A. & Horwitz, A.F. Integrin-ligand binding properties govern cell migration speed through cell-substratum adhesiveness. *Nature* **385**, 537-540 (1997).
165. Streuli, C.H. & Bissell, M.J. Expression of extracellular matrix components is regulated by substratum. *J Cell Biol* **110**, 1405-1415 (1990).
166. Massia, S.P. & Hubbell, J.A. An RGD spacing of 440 nm is sufficient for integrin alpha V beta 3-mediated fibroblast spreading and 140 nm for focal contact and stress fiber formation. *J Cell Biol* **114**, 1089-1100 (1991).
167. Ifkovits, J.L. & Burdick, J.A. Review: photopolymerizable and degradable biomaterials for tissue engineering applications. *Tissue Eng* **13**, 2369-2385 (2007).
168. Alcantar, N.A., Aydil, E.S. & Israelachvili, J.N. Polyethylene glycol-coated biocompatible surfaces. *J Biomed Mater Res* **51**, 343-351 (2000).
169. Phelps, E.A., *et al.* Maleimide cross-linked bioactive PEG hydrogel exhibits improved reaction kinetics and cross-linking for cell encapsulation and in situ delivery. *Adv Mater* **24**, 64-70, 62 (2012).
170. Lutolf, M.P. & Hubbell, J.A. Synthesis and physicochemical characterization of end-linked poly(ethylene glycol)-co-peptide hydrogels formed by Michael-type addition. *Biomacromolecules* **4**, 713-722 (2003).
171. Chiu, Y.C., Larson, J.C., Isom, A., Jr. & Brey, E.M. Generation of porous poly(ethylene glycol) hydrogels by salt leaching. *Tissue Eng Part C Methods* **16**, 905-912 (2010).
172. Keskar, V., Marion, N.W., Mao, J.J. & Gemeinhart, R.A. In vitro evaluation of macroporous hydrogels to facilitate stem cell infiltration, growth, and mineralization. *Tissue Eng Part A* **15**, 1695-1707 (2009).
173. Matson, J.B. & Stupp, S.I. Self-assembling peptide scaffolds for regenerative medicine. *Chem Commun* **48**, 26-33 (2012).
174. Arslan, E., Garip, I.C., Gulseren, G., Tekinay, A.B. & Guler, M.O. Bioactive Supramolecular Peptide Nanofibers for Regenerative Medicine. *Adv Healthc Mater* (2014).
175. Matson, J.B. & Stupp, S.I. Self-assembling peptide scaffolds for regenerative medicine. *Chem Commun (Camb)* **48**, 26-33 (2012).

176. Guler, M.O., *et al.* Presentation of RGDS epitopes on self-assembled nanofibers of branched peptide amphiphiles. *Biomacromolecules* **7**, 1855-1863 (2006).
177. Benoit, D.S.W. & Anseth, K.S. The effect on osteoblast function of colocalized RGD and PHSRN epitopes on PEG surfaces. *Biomaterials* **26**, 5209-5220 (2005).
178. Silva, G.A., *et al.* Selective differentiation of neural progenitor cells by high-epitope density nanofibers. *Science* **303**, 1352-1355 (2004).
179. Anderson, J.M., *et al.* Osteogenic differentiation of human mesenchymal stem cells synergistically enhanced by biomimetic peptide amphiphiles combined with conditioned medium. *Acta Biomater* **7**, 675-682 (2011).
180. Storrie, H., *et al.* Supramolecular crafting of cell adhesion. *Biomaterials* **28**, 4608-4618 (2007).
181. Galler, K.M., Aulisa, L., Regan, K.R., D'Souza, R.N. & Hartgerink, J.D. Self-assembling multidomain peptide hydrogels: designed susceptibility to enzymatic cleavage allows enhanced cell migration and spreading. *J Am Chem Soc* **132**, 3217-3223 (2010).
182. Sur, S., Matson, J.B., Webber, M.J., Newcomb, C.J. & Stupp, S.I. Photodynamic Control of Bioactivity in a Nanofiber Matrix. *Acs Nano* **6**, 10776-10785 (2012).
183. Kim, I.L., Khetan, S., Baker, B.M., Chen, C.S. & Burdick, J.A. Fibrous hyaluronic acid hydrogels that direct MSC chondrogenesis through mechanical and adhesive cues. *Biomaterials* **34**, 5571-5580 (2013).
184. Yoo, S.Y., Kobayashi, M., Lee, P.P. & Lee, S.W. Early osteogenic differentiation of mouse preosteoblasts induced by collagen-derived DGEA-peptide on nanofibrous phage tissue matrices. *Biomacromolecules* **12**, 987-996 (2011).
185. Anderson, J.M., *et al.* Osteogenic differentiation of human mesenchymal stem cells directed by extracellular matrix-mimicking ligands in a biomimetic self-assembled peptide amphiphile nanomatrix. *Biomacromolecules* **10**, 2935-2944 (2009).
186. Hennessy, K.M., *et al.* The effect of collagen I mimetic peptides on mesenchymal stem cell adhesion and differentiation, and on bone formation at hydroxyapatite surfaces. *Biomaterials* **30**, 1898-1909 (2009).
187. Karageorgiou, V. & Kaplan, D. Porosity of 3D biomaterial scaffolds and osteogenesis. *Biomaterials* **26**, 5474-5491 (2005).
188. Mastrogiacomo, M., *et al.* Role of scaffold internal structure on in vivo bone formation in macroporous calcium phosphate bioceramics. *Biomaterials* **27**, 3230-3237 (2006).
189. Hollister, S.J. Porous scaffold design for tissue engineering. *Nat Mater* **4**, 518-524 (2005).

190. Janmey, P.A. The cytoskeleton and cell signaling: component localization and mechanical coupling. *Physiol Rev* **78**, 763-781 (1998).
191. McBeath, R., Pirone, D.M., Nelson, C.M., Bhadriraju, K. & Chen, C.S. Cell shape, cytoskeletal tension, and RhoA regulate stem cell lineage commitment. *Dev Cell* **6**, 483-495 (2004).
192. Ceylan, H., *et al.* Bone-Like Mineral Nucleating Peptide Nanofibers Induce Differentiation of Human Mesenchymal Stem Cells into Mature Osteoblasts. *Biomacromolecules* (2014).
193. Shih, Y.R., Tseng, K.F., Lai, H.Y., Lin, C.H. & Lee, O.K. Matrix stiffness regulation of integrin-mediated mechanotransduction during osteogenic differentiation of human mesenchymal stem cells. *J Bone Miner Res* **26**, 730-738 (2011).
194. Shapiro, F. Bone development and its relation to fracture repair. The role of mesenchymal osteoblasts and surface osteoblasts. *Eur Cell Mater* **15**, 53-76 (2008).
195. Forgacs, G., Foty, R.A., Shafrir, Y. & Steinberg, M.S. Viscoelastic properties of living embryonic tissues: a quantitative study. *Biophys J* **74**, 2227-2234 (1998).
196. Mari-Buye, N., Luque, T., Navajas, D. & Semino, C.E. Development of a three-dimensional bone-like construct in a soft self-assembling peptide matrix. *Tissue Eng Part A* **19**, 870-881 (2013).
197. Wu, L.C., Yang, J. & Kopecek, J. Hybrid hydrogels self-assembled from graft copolymers containing complementary beta-sheets as hydroxyapatite nucleation scaffolds. *Biomaterials* **32**, 5341-5353 (2011).
198. Rnjak-Kovacina, J., *et al.* Tailoring the porosity and pore size of electrospun synthetic human elastin scaffolds for dermal tissue engineering. *Biomaterials* **32**, 6729-6736 (2011).
199. Xiao, J., *et al.* Construction of the recellularized corneal stroma using porous acellular corneal scaffold. *Biomaterials* **32**, 6962-6971 (2011).